Int J Hematol (2009) 89:716–717
DOI 10.1007/s12185-009-0322-5

LETTER TO THE EDITOR

Pneumocystis jiroveci pneumonia as an atypical presentation of X-linked agammaglobulinemia

Hirokazu Kanegane · Takashi Nakano · Yoshiki Shimono · Meina Zhao · Toshio Miyawaki

Received: 2 March 2009 / Revised: 9 April 2009 / Accepted: 10 April 2009 / Published online: 28 April 2009

X-linked agammaglobulinemia (XLA) is usually presented with clinical manifestations of bacterial respiratory and/or gastrointestinal infections below the age of 1 year, when the maternal IgG through placenta disappears from the circulation of the baby. Here, we describe an infant with XLA, who presented with interstitial pneumonia suggestive of *Pneumocystis jiroveci* (formerly *Pneumocystis carinii)* infection.

1 Patient report

A 3-month-old boy was admitted to Mie Hospital because of a long-standing cough, tachypnea and cyanosis. Physical examination showed a weight of 5.8 kg, temperature of 36.3°C, pulse of 170/min, respiration rate of 68/min, oxygen saturation on room air of 60%, respiratory retraction, and abnormal lung auscultation, but there was no lymphadenopathy. Chest radiology showed alveo-interstitial pneumonia (Fig. 1a), and chest computed tomography demonstrated diffuse ground-glass opacities (Fig. 1b). Laboratory tests showed a white blood count of 15,500/μl with 31.9% neutrophils and 54.4% lymphocytes, along with C-reactive protein of 0.02 mg/dl. The patient needed supplement oxygen, but did not require mechanical ventilation. He was first suspected of viral or *Chlamydia* pneumonia, and clarythromycin was administered but there was no improvement. Serum IgM against *Chlamydia trachomatis* and cytomegalovirus were negative. The patient's serum IgG, IgA and IgM levels were 108, 0 and 15 mg/dl, respectively, and the peripheral B cells were absent, suggesting an XLA despite the lack of a family history. With parental consent, the patient was diagnosed as having XLA based on a missense mutation (Arg28His) in the Bruton's tyrosine kinase (*BTK*) gene. The responses to phytohemagglutinin and concanavalin A are 56900 and 30900 cpm (control 141 cpm), respectively. Although T cell number and function were normal, he was suspected to have *Pneumocystis jiroveci* pneumonia. An elevated level of β-D glucan of >300 pg/ml (normal value <20) and KL-6 of 8750 U/ml (normal value, <500), suggested interstitial pneumonia caused by *Pneumocystis jiroveci*; however, polymerase chain reaction of sputum showed a negative result of *Pneumocystis jiroveci*. This may have been due to inadequate collection of sputum. He was treated with administration of sulfamethoxazole-trimethoprim (ST) and intravenous immunoglobulin (IVIG), with clinical improvement. The patient is currently well with IVIG replacement therapy and prophylactic administration of ST (Fig. 2).

2 Discussion

Interstitial pneumonia is caused by many organisms such as cytomegalovirus, adenovirus, fungus, and *Pneumocystis jiroveci*. An infant with interstitial pneumonia may be suspected of having an immunocompromised host with T cell deficiency, although there may have been *Pneumocystis jiroveci* pneumonia even in immunocompetent infants [1, 2]. XLA is a humoral immunodeficiency resulting from a block in early B cell development, and it is

H. Kanegane (✉) · M. Zhao · T. Miyawaki
Department of Pediatrics, Graduate School of Medicine, University of Toyama, 2630 Sugitani, Toyama, Toyama 930-0194, Japan
e-mail: kanegane@med.u-toyama.ac.jp

T. Nakano · Y. Shimono
Department of Pediatrics, Mie Hospital, Tsu, Japan

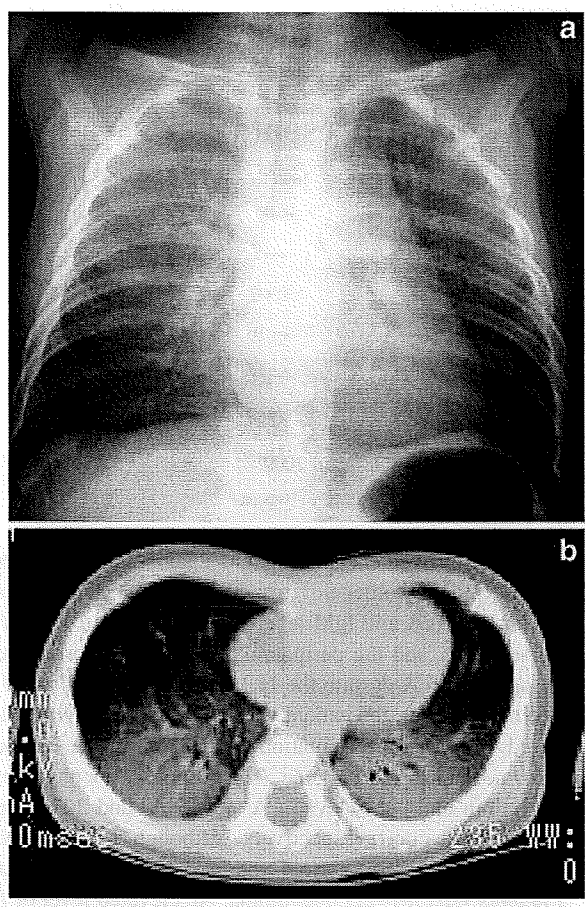

Fig. 1 Radiological findings in the patient. **a** Chest radiograph demonstrated bilateral perihilar opacities. **b** Computed tomography demonstrated diffuse ground-glass opacities in both lungs

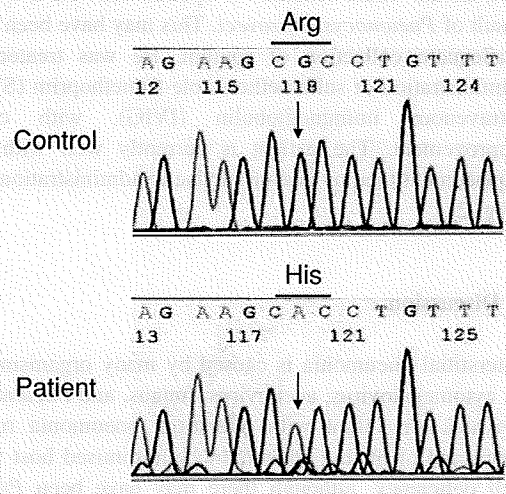

Fig. 2 *BTK* mutational analysis. DNA sequences of the exon 2 of the *BTK* gene in the patient and a control are shown. *Arrows* indicate position 215 in which the patient demonstrates a G to A mutation, indicating an amino acid substitution of Arg28His

clinically characterized by recurrent bacterial infections [3]. Although XLA patients sometimes demonstrate enteroviral infections, they usually show a normal response to viral and fungus infections because of normal T cell functions. However, 3 XLA patients with *Pneumocystis jiroveci* pneumonia have been reported [4–6]. One of these three was an adult receiving immunosuppressive therapy, but 2 patients were infants as in our case. It has recently been reported that Toll-like receptor signaling is impaired in XLA [7, 8] and that may be associated with the development of *Pneumocystis jiroveci* infection in XLA patients. Prophylactic administration of ST as well as IVIG replacement therapy would be recommended for the treatment of XLA patients.

Acknowledgments This study was partly supported by the Ministry of Education, Culture, Sports, Science and Technology of Japan, and Ministry of Health, Labour and Welfare of Japan.

References

1. Stagno S, Pifer LL, Hughes WT, Brasfield DM, Tiller RE. *Pneumocystis carinii* pneumonitis in young immunocompetent infants. Pediatrics. 1980;66:56–62.
2. Brasfield DM, Stagno S, Whitley RJ, Cloud G, Cassell G, Tiller RE. Infant pneumonitis associated with cytomegalovirus, *Chlamydia*, *Pneumocystis*, and *Ureaplasma*: follow-up. Pediatrics. 1987;79:76–83.
3. Conley ME, Broides A, Hernandez-Trujillo V, Howard V, Kanegane H, Miyawaki T, et al. Genetic analysis of patients with defects in early B-cell development. Immunol Rev. 2005;203:216–34. doi:10.1111/j.0105-2896.2005.00233.x.
4. Alibrahim A, Lepore M, Lierl M, Fillipovich A, Assa'ad A. *Pneumocystis carinii* pneumonia in an infant with X-linked agammaglobulinemia. J Allergy Clin Immunol. 1998;101:552–3. doi:10.1016/S0091-6749(98)70363-X.
5. Gaspar HB, Ferrando M, Caragol I, et al. Kinase mutation Btk results in atypical X-linked agammaglobulinemia phenotype. Clin Exp Immunol. 2000;120:346–50. doi:10.1046/j.1365-2249.2000.01230.x.
6. Sirianni MC, Atzori C, De Santis W, et al. A case of *Pneumocystis jiroveci* pneumonia in X-linked agammaglobulinemia treated with immunosuppressive therapy: a lesson for immunologists. Int Arch Allergy Immunol. 2005;140:82–8. doi:10.1159/000092139.
7. Sochorová K, Horáth R, Rozková D, et al. Impaired Toll-like receptor 8-mediated IL-6 and TNF-alpha production in antigen-presenting cells from patients with X-linked agammaglobulinemia. Blood. 2007;109:253–2556. doi:10.1182/blood-2006-07-037960.
8. Taneichi H, Kanegane H, Sira MM, et al. Toll-like receptor signaling is impaired in dendritic cells from patients with X-linked agammaglobulinemia. Clin Immunol. 2008;126:148–54. doi:10.1016/j.clim.2007.10.005.

Published June 1, 2009

JEM

ARTICLE

Molecular explanation for the contradiction between systemic Th17 defect and localized bacterial infection in hyper-IgE syndrome

Yoshiyuki Minegishi,[1] Masako Saito,[1] Masayuki Nagasawa,[2] Hidetoshi Takada,[3] Toshiro Hara,[3] Shigeru Tsuchiya,[4] Kazunaga Agematsu,[5] Masafumi Yamada,[6] Nobuaki Kawamura,[6] Tadashi Ariga,[6] Ikuya Tsuge,[7] and Hajime Karasuyama[1]

[1]Department of Immune Regulation and [2]Department of Pediatrics and Developmental Biology, Graduate School, Tokyo Medical and Dental University, Tokyo 113-8519, Japan
[3]Department of Pediatrics, Graduate School of Medical Sciences, Kyushu University, Fukuoka 812-0054, Japan
[4]Department of Pediatrics, Tohoku University, Sendai 980-0872, Japan
[5]Department of Pediatrics, Shinshu University, Matsumoto 390-8621, Japan
[6]Department of Pediatrics, Hokkaido University Graduate School of Medicine, Sapporo 060-8638, Japan
[7]Department of Pediatrics, Fujita Health University, Nagoya 470-1192, Japan

Hyper-IgE syndrome (HIES) is a primary immunodeficiency characterized by atopic manifestations and susceptibility to infections with extracellular pathogens, typically *Staphylococcus aureus*, which preferentially affect the skin and lung. Previous studies reported the defective differentiation of T helper 17 (Th17) cells in HIES patients caused by hypomorphic *STAT3* mutations. However, the apparent contradiction between the systemic Th17 deficiency and the skin/lung-restricted susceptibility to staphylococcal infections remains puzzling. We present a possible molecular explanation for this enigmatic contradiction. HIES T cells showed impaired production of Th17 cytokines but normal production of classical proinflammatory cytokines including interleukin 1β. Normal human keratinocytes and bronchial epithelial cells were deeply dependent on the synergistic action of Th17 cytokines and classical proinflammatory cytokines for their production of antistaphylococcal factors, including neutrophil-recruiting chemokines and antimicrobial peptides. In contrast, other cell types were efficiently stimulated with the classical proinflammatory cytokines alone to produce such factors. Accordingly, keratinocytes and bronchial epithelial cells, unlike other cell types, failed to produce antistaphylococcal factors in response to HIES T cell–derived cytokines. These results appear to explain, at least in part, why HIES patients suffer from recurrent staphylococcal infections confined to the skin and lung in contrast to more systemic infections in neutrophil-deficient patients.

CORRESPONDENCE
Yoshiyuki Minegishi:
yminegishi.mbch@tmd.ac.jp

Abbreviations used: BD, β-defensin; CAA, *Candida albicans* antigen; CGD, chronic granulomatous disease; HIES, hyper-IgE syndrome; HMVEC-L, human lung microvascular endothelial cell; HUVEC, human umbilical vein endothelial cell; SEB, staphylococcal enterotoxin B; TLR, Toll-like receptor.

The identification of Th17 cells as a third subset of helper T cells has illuminated the fact that distinct subsets of helper T cells have been evolved to protect our body from infections by various types of microorganisms and are involved differently in the induction and exacerbation of various immunological disorders. Th17 cells are characterized and distinguished from IFN-γ–producing Th1 cells and IL-4–producing Th2 cells by their production of so-called Th17 cytokines including IL-17 (IL-17A), IL-17F, and IL-22 (1–4). For their differentiation from naive CD4 T cells, Th17 cells require different cytokines and transcription factors than do Th1, Th2, or regulatory T cells. The roles of Th17 cells in immune responses are also different from those of other helper T cells. In particular, their pathological roles in autoimmune and inflammatory diseases, including multiple sclerosis, rheumatoid arthritis, psoriasis, and inflammatory bowel diseases, have been studied extensively (5–10).

Although the functions of Th17 cells under physiological conditions have not been completely elucidated, accumulating data suggest that Th17 cells play crucial roles in the host defense against extracellular pathogens that are

The Rockefeller University Press $30.00
J. Exp. Med. Vol. 206 No. 6 1291-1301
www.jem.org/cgi/doi/10.1084/jem.20082767

Supplemental Material can be found at:
http://jem.rupress.org/cgi/content/full/jem.20082767/DC1

Published June 1, 2009
JEM

not efficiently cleared by Th1- and Th2-type immune responses. Th17-type cytokines IL-17A and IL-17F are important for the recruitment of neutrophils (11), whereas IL-22 induces the production of antimicrobial peptides β-defensin (BD) 2 and BD3 by keratinocytes, through the activation of STAT3 (12–14). Mice with a homozygous deletion of the gene encoding the IL-17RA (IL-17 receptor A) and mice that do not produce IL-22 are susceptible to lung infection by the Gram-negative bacteria *Klebsiella pneumoniae* and *Mycoplasm pulmonis* (15–17). Mice that produce neither IL-17A nor IL-17F are susceptible to skin infection by the Gram-positive bacteria *Staphylococcus aureus* (18). Administration of anti–IL-17A neutralizing antibodies impairs both the intra-abdominal abscess formation in response to *Bacteroides fragilis* and *Escherichia coli* (19–21) and the host defense against systemic infection by the fungus *Candida albicans* (22). These data indicate that Th17 cells play a key role in immune responses to extracellular bacteria and fungi in mice. In contrast, the anti-pathogenic roles of Th17 cells in humans are relatively uncertain.

Recent studies demonstrated that the differentiation of human Th17 cells was defective in patients with hyper-IgE syndrome (HIES) (23–26). HIES is a primary immunodeficiency disease caused by dominant-negative mutations in the DNA-binding domain, SH2 domain, or transactivating domain of STAT3 (26–28). As expected from the important roles of STAT3 in transducing signals for a variety of cytokines, growth factors, and hormones, patients with HIES display complex clinical manifestations in multiple organs, including atopic dermatitis with high serum IgE levels and abnormalities of the bones and teeth (29–32). Most patients suffer from recurrent infections by fungi and bacteria, predominantly the Gram-positive bacteria *S. aureus*. The presence of these infections suggests that Th17 cells play a crucial role in protection from extracellular pathogens, not only in mice but also in humans. However, curiously, the staphylococcal infections in HIES patients are often confined to the skin and lung and manifest clinically as skin abscesses and cyst-forming pneumonia. These skin- and lung-restricted infections are in sharp contrast to the pattern of infection observed in patients with a neutrophil deficiency. For example, in patients with chronic granulomatous disease (CGD), staphylococcal infections occur in a wide variety of organs including the lung, lymph nodes, skin, liver, bone, gastrointestinal tract, kidney, and brain (33). Thus, it remains elusive why HIES patients suffer from skin- and lung-restricted staphylococcal infections in spite of their systemic Th17 deficiency.

In the present study, we explored possible molecular mechanisms underlying the recurrent staphylococcal infections confined to the skin and lung in HIES patients. We found that primary human keratinocytes and bronchial epithelial cells displayed a much stronger dependence than other cell types on Th17 cytokines in their production of antistaphylococcal factors including the neutrophil-recruiting chemokines and antibacterial peptides. T cells from HIES patients, in spite of their defect in production of Th17 cytokines, showed normal production of other proinflammatory cytokines, including IL-1β, which was insufficient for triggering keratinocytes and bronchial epithelial cells but sufficient for other cell types to produce antistaphylococcal factors. Th17 cytokines and classical proinflammatory cytokines synergistically stimulated keratinocytes and bronchial epithelial cells, but the synergy was not seen in other types of cells. These findings provide a possible molecular explanation for the apparent contradiction between the systemic Th17 deficiency and the skin and lung-restricted staphylococcal infections in HIES patients.

RESULTS

HIES T cells produce little or no Th17 cytokines and fail to stimulate keratinocytes to secrete neutrophil-recruiting chemokines and BDs

We first examined the profile of cytokines produced by T cells from our cohort of HIES patients whose *STAT3* genes carried mutations. The amounts of IL-17A and IL-22 secreted from the patients' T cells upon stimulation with anti-CD3 and anti-CD28 mAbs were invariably only ~5–10% of those from healthy control subjects, which is in accordance with previous results (23–26), whereas the production levels of IFN-γ, IL-1β, and TNF-α were comparable in the two groups (Fig. 1). Real-time quantitative RT-PCR demonstrated that the up-regulation of *IL-17F* expression by the patients' T cells was also impaired (unpublished data). Thus, the patients' T cells showed a selective defect in the production of Th17 cytokines.

We next investigated the functional consequences of the Th17 deficiency in the context of staphylococcal infections of the skin. Normal human primary epidermal keratinocytes were cultured in vitro with culture supernatants from HIES patients' or control subjects' T cells that had been unstimulated or stimulated with anti-CD3 plus anti-CD28. The expression and production of two chemokines, CXCL8 (IL-8) and CCL2, was up-regulated in the keratinocytes cultured with the conditioned medium from activated control T cells (Fig. 2 A and Fig. S1). In contrast, although CCL2 was also up-regulated by the conditioned medium from activated HIES T cells, CXCL8 was not (Fig. 2 A and Fig. S1). Among the three antimicrobial peptides (BDs) examined, at the mRNA and protein level the expression of BD1 but not BD2 or BD3 was up-regulated in keratinocytes when they were stimulated with conditioned medium from the T cells of HIES patients, but all three were up-regulated by the conditioned medium from the control subjects' T cells (Fig. 2 A and Fig. S1). Thus, the HIES patients' T cells could not stimulate keratinocytes to produce a significant amount of the neutrophil-recruiting chemokine CXCL8 or the antimicrobial peptides BD2 and BD3, but they could stimulate the up-regulation of CCL2 and BD1.

T cell–derived Th17 cytokines are responsible for the production of CXCL8 and BDs from keratinocytes

When the supernatants from activated control T cells were treated with the combination of anti–IL-17A and anti–IL-22 blocking mAbs before incubation with keratinocytes, their capability of stimulating keratinocytes to up-regulate CXCL8, BD2, and BD3 was diminished to the level displayed by the

Published June 1, 2009

HIES patients' T cells (Fig. 2 A and Fig. S1). Either anti–IL-17A or anti–IL-22 alone was less effective than their combination (Fig. S2). Thus, the defective production of chemokines and BDs by keratinocytes in response to the conditioned medium from the patients' T cells was attributable to the T cells' defective production of Th17 cytokines.

We next examined the direct effect of the keratinocyte-derived factors on the growth of *Staphylococcus aureus* using a colony-forming assay (Fig. 2, B and C). When bacteria were cultured with the culture supernatant from keratinocytes stimulated by control T cells, the number of bacterial colonies was reduced to 60% as compared with that when cultured with control medium. However, this was not the case when HIES T cells were used to stimulate keratinocytes. The antibacterial activity was completely abrogated when the culture supernatant from the control T cells was pretreated with the blocking mAbs for IL-17A and IL-22 before it was added to the keratinocytes (Fig. 2 B), and it was attenuated when the keratinocyte supernatants were pretreated with an anti-BD3 mAb before their application to the bacterial culture (Fig. 2 C). These results indicated that control but not HIES T cells produced Th17 cytokines that, in turn, acted on keratinocytes to elicit their secretion of antimicrobial factors including BD3.

Keratinocytes and bronchial epithelial cells display a greater dependence on Th17 cytokines for their production of chemokines and BDs than other cell types

To learn why the staphylococcal infections are confined to the skin and lung in HIES patients, we analyzed different lineages of human primary cells for their ability to secrete chemokines and BDs in response to T cell–derived factors including Th17 cytokines. We first compared their responsiveness to culture supernatants from either control or patient T cells that were activated with anti-CD3 and anti-CD28 mAbs. Primary bronchial epithelial cells responded to the T cell conditioned medium just as the primary keratinocytes did. That is, both cell types up-regulated the expression and production of chemokines (CXCL8 and CXCL1) and BDs (BD2 and BD3) when incubated with the supernatants from control T cells but not from HIES T cells (Fig. 3 A and Fig. S3). Interestingly, primary dermal fibroblasts, human umbilical vein endothelial cells (HUVEC), and human lung microvascular endothelial cells (HMVEC-L) responded equally well, in terms of their secretion of the chemokines and BDs, to the supernatants from control or patient T cells (Fig. 3 A and Fig. S3). This was also true for the expression and production of CXCL8 and CXCL1 by human macrophages (Fig. 3 A and Fig. S3). Human macrophages did not produce detectable amounts of BDs. Thus, keratinocytes and bronchial epithelial cells responded differently to T cell–derived factors than the other cell types tested and appeared to be much more dependent on Th17 cytokines for their induction to secrete chemokines and BDs.

These findings prompted us to examine the responses of different cell types to individual cytokines and their combinations, including the Th17 cytokines (IL-17A, IL-17F, and IL-22), classical proinflammatory cytokines (IL-1β, TNF-α, and IFN-γ), or both. Keratinocytes secreted CXCL8 in response to IL-17A, IL-22, IL-1β, or TNF-α in a dose-dependent

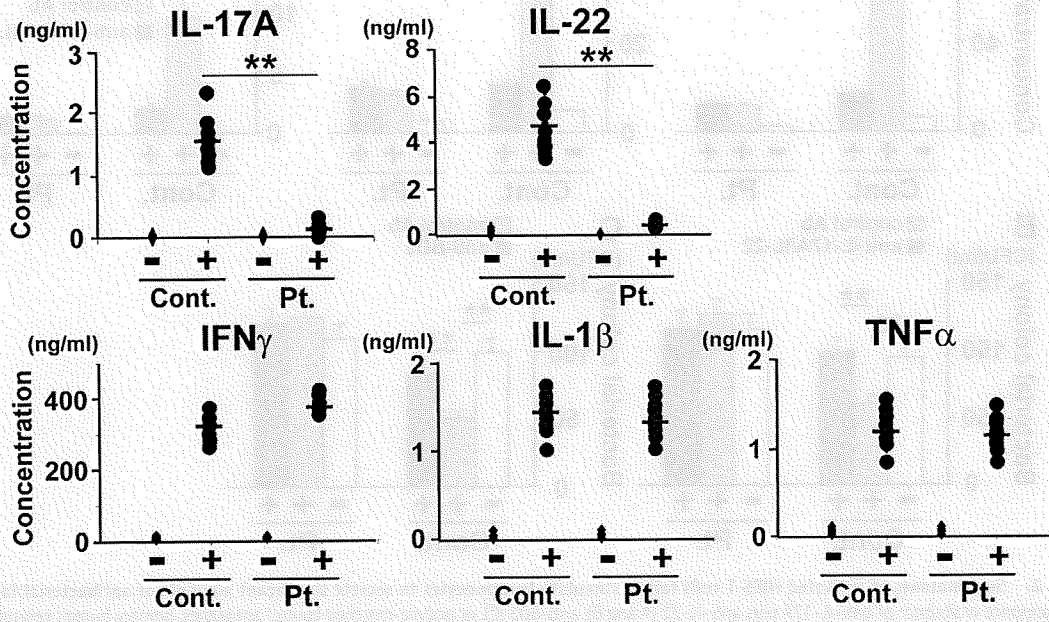

Figure 1. HIES T cells produce greatly reduced amounts of Th17 cytokines and normal amounts of classical proinflammatory cytokines upon activation. PBMCs from HIES patients (Pt.) and control subjects (Cont.; $n = 8$ each, indicated by dots) were stimulated (+) or not (−) with anti-CD3 and anti-CD28 for 72 h, and the concentration of the indicated cytokines in their culture supernatants was determined by ELISA. The results shown are representative of three independent experiments. **, $P < 0.01$.

Published June 1, 2009

manner, but they responded poorly to IL-17F and IFN-γ (Fig. S4 A). Using the Th17 cytokine cocktail or the classical proinflammatory cytokine cocktail resulted in some additive effect on the keratinocytes' secretion of CXCL8 (Fig. S4, B and C). In contrast, the combination of both types of cytokines dramatically enhanced the CXCL8 production by the keratinocytes (Fig. 3 B and Fig. S5). This was also the case for bronchial epithelial cells (Fig. 3 B). In contrast, fibroblasts, HUVEC, and HMVEC-L secreted a large quantity of CXCL8 in response to the classical proinflammatory cytokine cocktail, but the further addition of Th17 cytokine cocktail caused no significant enhancement of CXCL8 production (Fig. 3 B). Furthermore, the Th17 cytokine cocktail was much less effective in stimulating fibroblasts, HUVEC, and HMVEC-L than the classical cytokine cocktail, and the amount of CXCL8 produced by the Th17 cytokine cocktail-treated fibroblasts, HUVEC, and HMVEC-L was ~10–30% of that produced by stimulation with the classical proinflammatory cocktail. Macrophages responded to the cytokines in a pattern similar to fibroblasts, HUVEC, and HMVEC-L, although the macrophages produced 10× less CXCL8 than the others.

In keratinocytes and bronchial epithelial cells, the marked synergy caused by combining the Th17 and classical proinflammatory cytokines affected not only the expression of CXCL8 but also that of other chemokines (CXCL1 and CXCL2) and BDs (BD2 and BD3; Fig. S6 A). In accordance with this finding, the supernatants of keratinocytes stimulated with the Th17–classical cytokine combination caused robust neutrophil chemotaxis compared with the supernatants from keratinocytes stimulated with only one of the cocktails (Fig. S6 B).

Previous studies demonstrated that the stimulation of keratinocytes with toll-like receptor (TLR) 2 ligands induces the production of the chemokines and antimicrobial peptides (34, 35). In agreement with this, the keratinocytes showed up-regulated CXCL8 secretion and BD expression in response to lipoteichoic acid, peptidoglycan, or fixed *S. aureus*, but the extent of up-regulation was <10% of that observed after stimulation with the combination of Th17 and proinflammatory cytokines (Fig. S6 C).

Molecular mechanisms underlying the unique responsiveness of keratinocytes and bronchial epithelial cells to Th17 cytokines in synergy with other proinflammatory cytokines

To explore the possible molecular basis of the poorer response of keratinocytes and bronchial epithelial cells to the

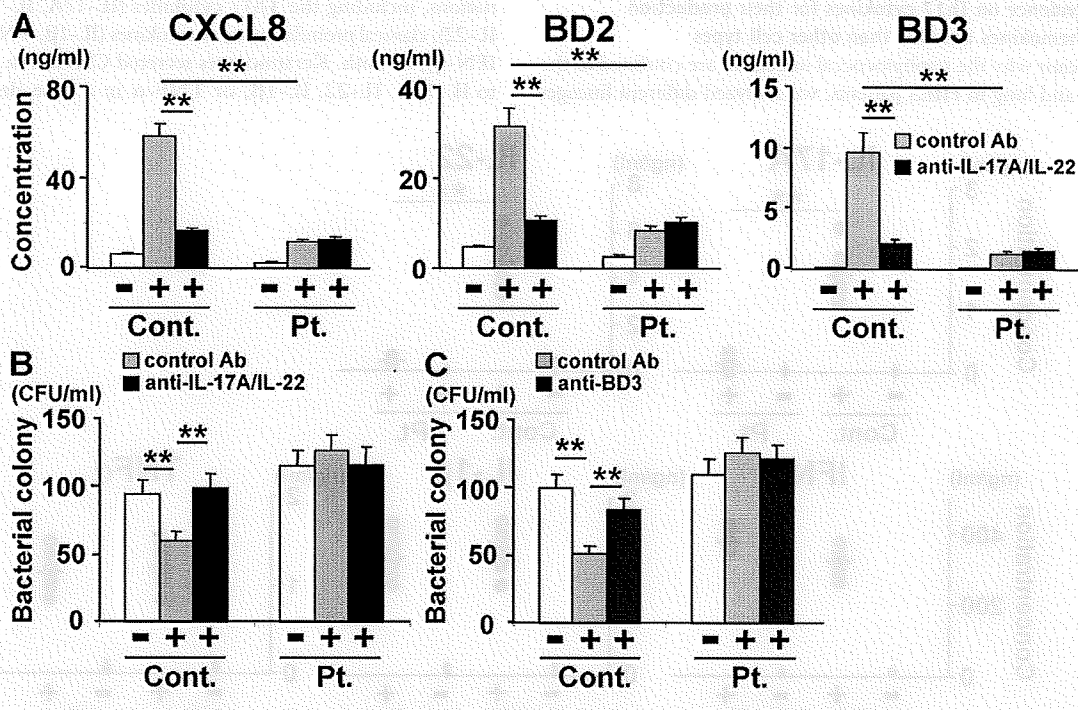

Figure 2. Supernatants of activated HIES T cells fail to stimulate keratinocytes to secrete significant amounts of antibacterial factors. In the presence or absence of anti–IL-17A plus anti–IL-22 (A and B), anti-BD3 (C), or isotype-matched control antibodies, primary human keratinocytes were incubated for 48 h with the supernatants of HIES (Pt.) or control (Cont.) T cells that had been stimulated (+) or not (−) with anti-CD3 and anti-CD28 for 72 h as in Fig. 1. (A) The concentration of CXCL8, BD2, and BD3 in keratinocytes supernatants was determined by ELISA. Representative data from one patient and one control are shown (mean ± SD; $n = 3$), and similar results were obtained from the other patients and controls. (B and C) The culture supernatants of keratinocytes were analyzed for their antistaphylococcal activity by the colony assay (mean ± SD; $n = 3$). The results shown in are representative of at least three independent experiments. **, $P < 0.01$.

Published June 1, 2009

classical proinflammatory cytokines, as compared with the other types of cells, we analyzed the expression of the classical cytokine IL-1R1 (IL-1 receptor) and its antagonists IL-1R2 and IL-1Ra (Fig. 4, A and B). Compared with fibroblasts, keratinocytes expressed 1/600th of IL-1R1 transcripts, 170-fold more IL-1Ra transcripts, and 260-fold more IL-1R2 (Fig. 4 A). The great difference in their expression between keratinocytes and fibroblasts was also confirmed at the protein level (Fig. 4 B). Bronchial epithelial cells showed the keratinocyte-type expression, whereas HUVEC and HMVEC-L displayed the fibroblast-type expression (Fig. 4 A and not depicted). Consistent with this result, keratinocytes showed a much poorer up-regulation of c-Fos and IL-6 than fibroblasts in response to IL-1β (Fig. 4 C). This appeared to partly explain why keratinocytes and bronchial epithelial cells were less sensitive to the classical proinflammatory cytokines than fibroblasts but did not account for the strong synergy between the Th17 and the classical proinflammatory cytokines in the keratinocytes. Therefore, we next examined the possible cross-talk between the two types of cytokines in terms of the regulation of cytokine receptor expression.

We found that the expression of the Th17 cytokine receptors IL-17RA, IL-17RC, and IL-22R was up-regulate, in keratinocytes incubated with the classical proinflammatory

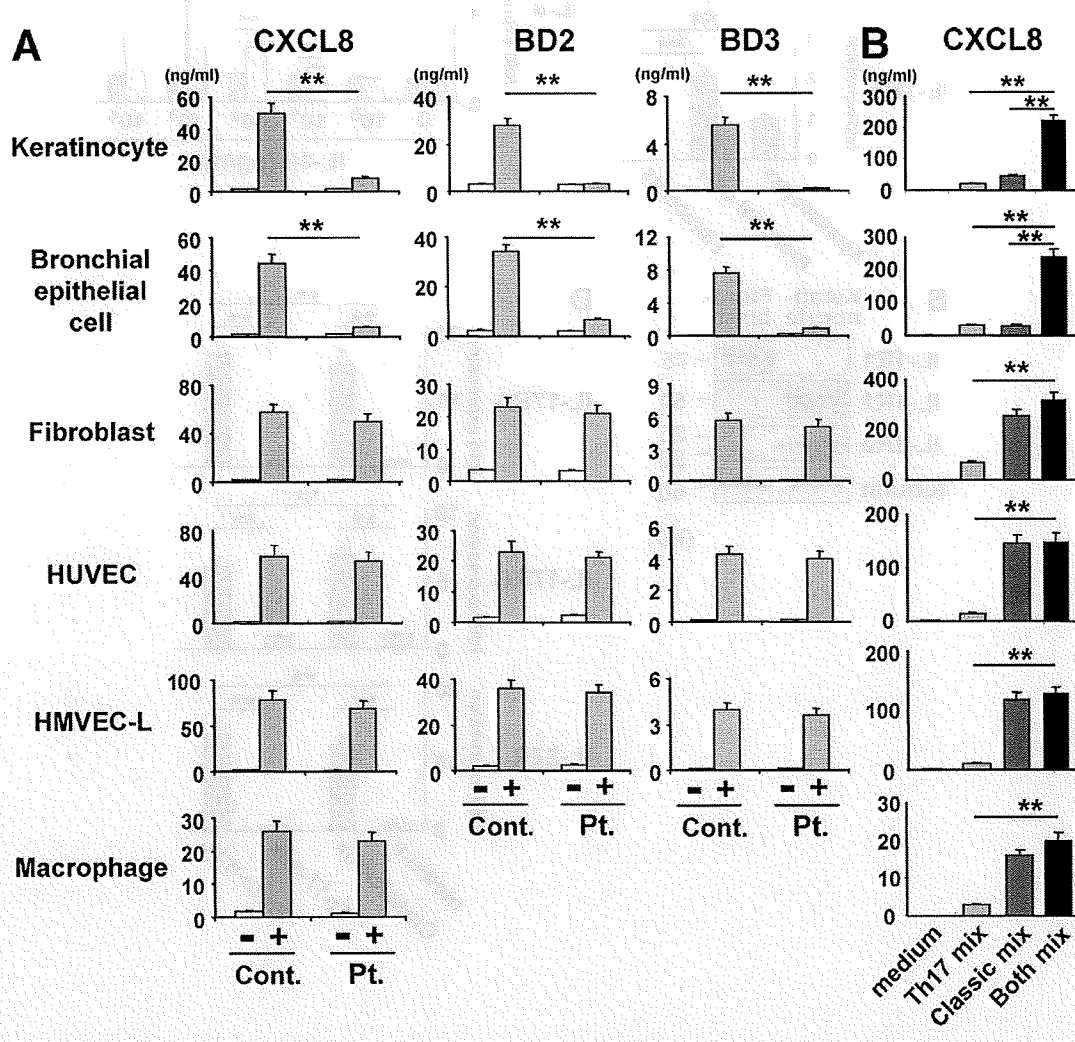

Figure 3. Keratinocytes and bronchial epithelial cells show greater dependence on Th17 cytokines for the production of chemokines and BDs than other cell types. Primary human keratinocytes, bronchial epithelial cells, dermal fibroblasts, endothelial cells (HUVEC and HMVEC-L), and macrophages were incubated for 48 h with T cell supernatants that were prepared as described in Fig. 1 A or with the Th17 cytokine cocktail (Th17 mix: IL-17A + IL-17F + IL-22), the classical proinflammatory cytokine cocktail (classical mix: TNF-α + IL-1β + IFN-γ), or the combination of both (both mix; B). The concentration of CXCL8, BD2, and BD3 in their culture supernatants was determined by ELISA. Representative data from one patient and one control are shown in A (mean ± SD; $n = 3$), and similar results were obtained from the other patients and controls. The results shown are representative of at least three independent experiments. **, $P < 0.01$.

Published June 1, 2009

JEM

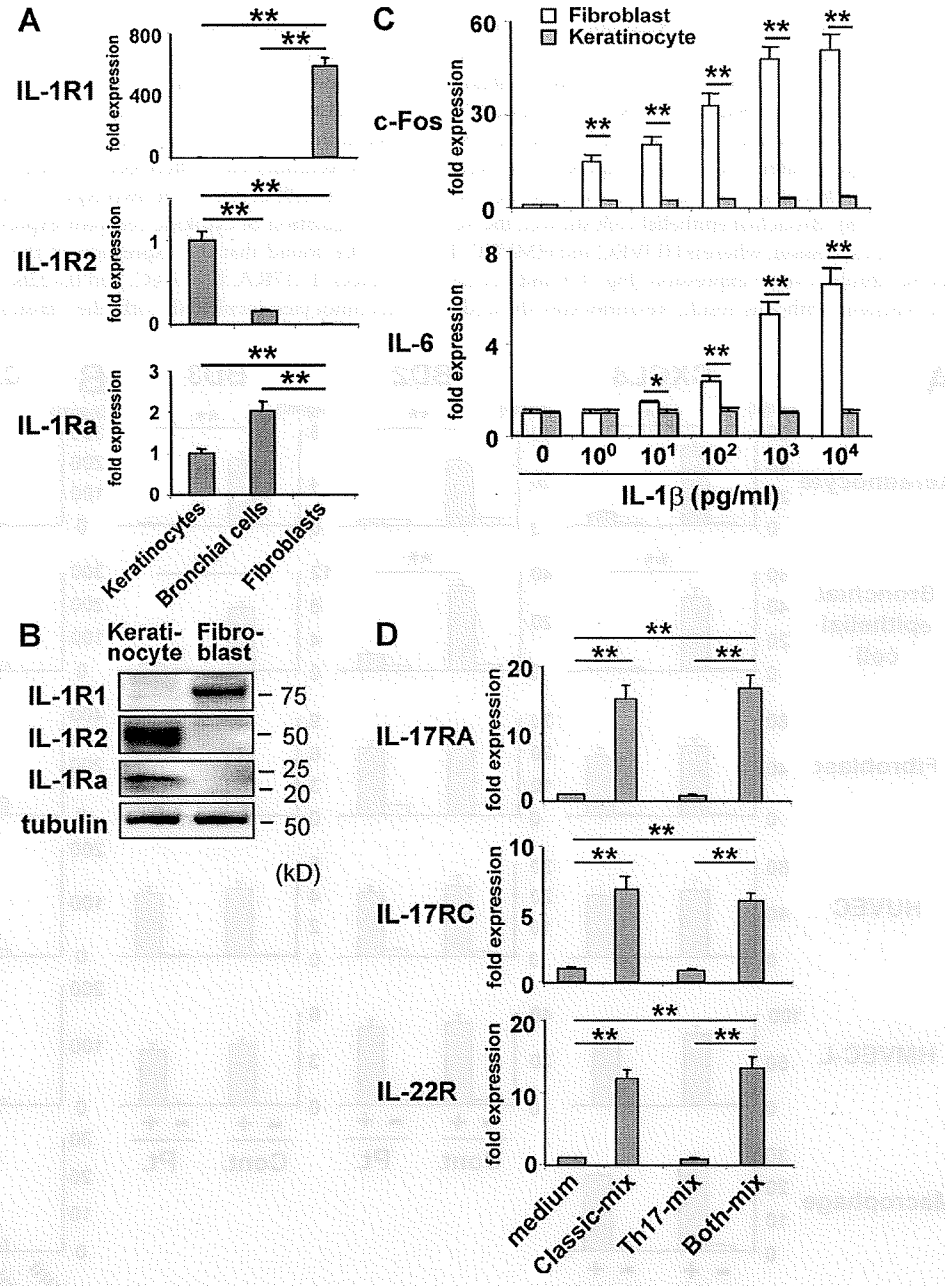

Figure 4. Distinct expression and regulation of the cytokine receptors in keratinocytes and fibroblasts compared with those in other cell types. (A) The expression of *IL-1R1*, *IL-1Ra*, and *IL-1R2* in the indicated cells was determined by quantitative RT-PCR. Data shown were normalized to *HPRT* levels, and the level of expression in keratinocytes was defined as 1.0. (B) IL-1R1, IL-1R2, and IL-1Ra proteins in keratinocytes and fibroblasts were detected by immunoblotting. (C) Keratinocytes and fibroblasts were cultured for 15 min with the indicated concentration of IL-1β and analyzed by quantitative RT-PCR for the expression of *c-Fos* and *IL-6*. Data shown were normalized to HPRT levels, and the level of expression in cells cultured without IL-1β was defined as 1.0 for each cell type. (D) Keratinocytes cultured as in Fig. 3 B were analyzed by quantitative RT-PCR for the expression of *IL-17RA*, *IL-17RC*, and *IL-22R*. The data shown were normalized to the *HPRT* levels, and the level of expression in cells cultured without any added cytokine was defined as 1.0. The results shown are representative of three independent experiments. Error bars show mean ± SD ($n = 3$). *, $P < 0.05$; **, $P < 0.01$.

Published June 1, 2009

cytokines but not the Th17 cytokines (Fig. 4 D and Fig. S7). Conversely, in keratinocytes incubated with the Th17 cytokines, the expression of the receptors for the classical proinflammatory cytokines was up-regulated, albeit less markedly (unpublished data). This reciprocal up-regulation of cytokine receptor expression was also observed in bronchial epithelial cells (unpublished data). These findings could account, at least in part, for the synergistic effect of the Th17 and the classical proinflammatory cytokines on the production of antibacterial factors by keratinocytes and bronchial epithelial cells.

HIES T cells show poor ability of stimulating keratinocytes in response to staphylococcal superantigens and candida antigens

We next investigated the responses of HIES T cells under more clinically relevant conditions to obtain a better insight into the susceptibility to staphylococcal infections observed in HIES patients. When stimulated with the *S. aureus*–derived superantigens for T cells, staphylococcal enterotoxin B (SEB), HIES patients' T cells produced drastically reduced amounts of IL-17A and IL-22, <10% of those produced by control T cells (Fig. 5 A). In contrast, the IL-1β production was normal, and the IFN-γ and TNF-α production was even enhanced in SEB-stimulated HIES T cells (Fig. 5 A). It is of note that the supernatants of SEB-stimulated HIES T cells showed much poorer ability to induce the production of CXCL8 and BD2 in keratinocytes compared with those from control T cells (Fig. 5 B). In contrast, both supernatants from HIES and control T cells almost equally well stimulated fibroblasts to produce CXCL8 and BD2. The combination of anti–IL-17A and –IL-22 efficiently inhibited the CXCL8/BD2-inducing activity of control T cells' supernatants in keratinocytes but showed no significant inhibition in the CXCL8/BD2 production from fibroblasts that were stimulated with the supernatants from either control or HIES T cells (Fig. 5 B). These results strongly suggested that Th17

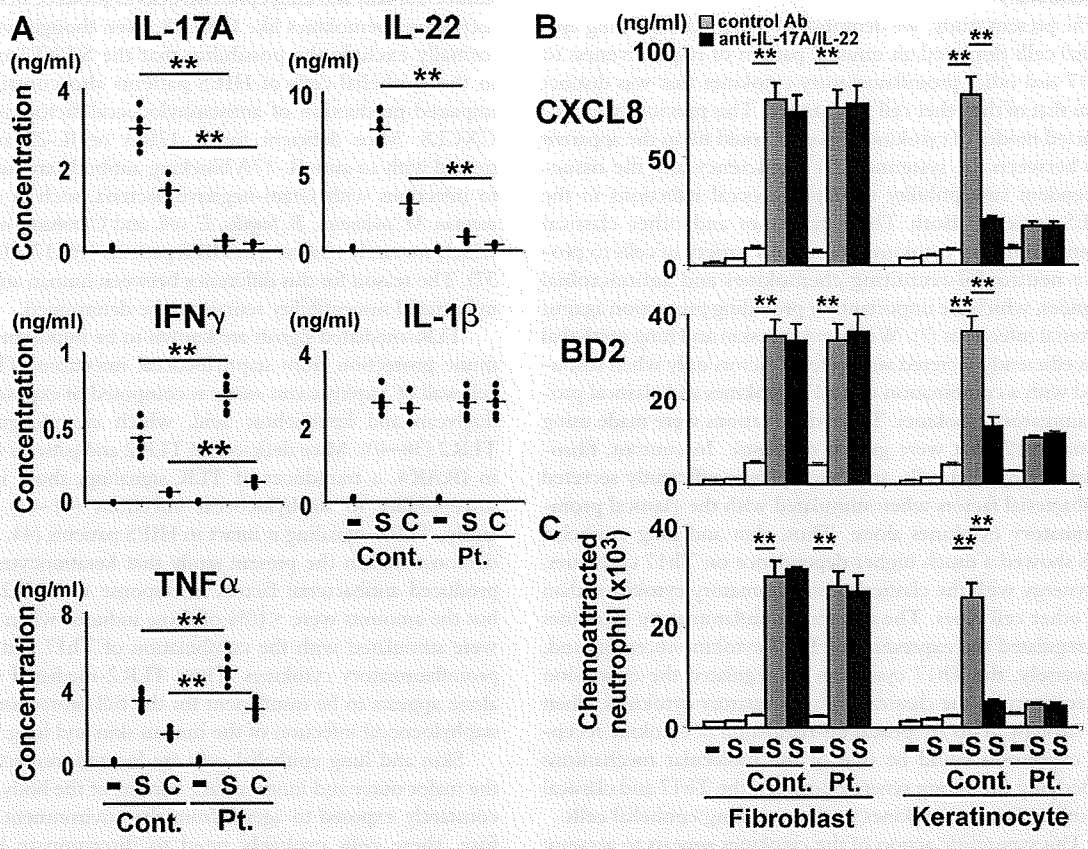

Figure 5. HIES T cells show poor ability of stimulating keratinocytes in response to staphylococcal superantigens and candida antigens. (A) PBMCs from HIES patients (Pt.) and control subjects (Cont.; $n = 6$ each, indicated by dots) were stimulated or not (−) with SEB (S, 100 ng/ml) or CAA (C, 1/20,000 vol/vol) for 5 d, and the concentration of the indicated cytokines in their culture supernatant was determined by ELISA. (B and C) Fibroblasts and keratinocytes were cultured for 48 h in the absence (−) or presence (S) of SEB or with the supernatants of patients (Pt.) or control (Cont.) PBMCs that had been unstimulated (−) or stimulated with SEB (S) as in A, in the presence or absence of anti–IL-17A + anti–IL-22 or isotype-matched control antibodies. Their culture supernatants were analyzed by ELISA for the secretion of CXCL8 and BD2 (B) and evaluated for their neutrophil chemotactic activity (C). The results shown are representative of two independent experiments. Error bars show mean ± SD ($n = 3$). **, $P < 0.01$.

Published June 1, 2009

cytokines secreted by SEB-stimulated T cells played a critical role in the induction of CXCL8 and BD2 production in keratinocytes but not in fibroblasts. In accord with these results, supernatants of keratinocytes stimulated with HIES T cells showed little or no ability of neutrophil chemoattraction, whereas those of keratinocytes stimulated with control T cells and those of fibroblasts stimulated with either control or HIES T cells induced robust neutrophil chemotaxis (Fig. 5 C). These in vitro findings may account in part, if not entirely, for the skin/lung-confined susceptibility to staphylococcal infections observed in HIES patients.

We further examined the responsiveness of HIES T cells to *Candida albicans* antigen (CAA). HIES T cells showed impaired cytokine production in response to CAA in the essentially same pattern as observed in response to SEB (Fig. 5 A). This may also explain in part the incidence of mucocutaneous infections with *C. albicans* that is often observed in HIES patients.

DISCUSSION

In the present study, we demonstrated that skin and lung epithelial cells displayed an unusual pattern of responsiveness to Th17 and other proinflammatory cytokines that was distinct from that of the other cell types tested. This previously unrecognized modes of cytokine responses could fill in the apparent gap between the systemic Th17 deficiency and the tissue-dependent susceptibility to staphylococcal infections in the HIES patients. Both Th17 cytokines and other classical proinflammatory cytokines stimulate a variety of cells to produce neutrophil-recruiting chemokines and antimicrobial peptides, which are important for providing protection against bacterial infections (7). We found that skin and lung epithelial cells efficiently secreted antibacterial factors only when stimulated with a combination of Th17 cytokines and classical proinflammatory cytokines. These observations were made using primary cells that were grown on plastic. In contrast, fibroblasts, endothelial cells, and macrophages efficiently secreted antibacterial factors when stimulated with the classical proinflammatory cytokines alone. Thus, skin and lung epithelial cells showed a much higher dependence on Th17 cytokines, in synergy with the classical proinflammatory cytokines, than the other cell types. The classical proinflammatory cytokines up-regulated the expression of Th17 cytokine receptors and, conversely, the Th17 cytokines up-regulated the expression of receptors for the classical proinflammatory cytokines, albeit less strongly. This reciprocal up-regulation of cytokine receptor expression could be one of the molecular mechanisms underlying the strong synergy between the Th17 and classical proinflammatory cytokines in skin and lung epithelial cells.

This synergistic action of the cytokines appears to account in part, if not entirely, for the skin- and lung-restricted staphylococcal infections of HIES patients. *S. aureus* produces enterotoxins, including SEB, that function as superantigens to stimulate the bulk of T cells. The HIES patients' T cells showed impaired production of Th17 cytokines in response to SEB but normal production of the classical proinflammatory cytokines. Therefore, the skin and lung epithelial cells of HIES patients, unlike other cell types, probably do not secrete sufficient amounts of neutrophil-recruiting chemokines and the antimicrobial peptide BDs to fend off staphylococcal infection. With regard to the sites of bacterial infections, it is important to consider the pathogen's characteristics. The tendency of *S. aureus* to colonize the skin and upper respiratory tract may explain the skin/lung-restricted staphylococcal infections observed in HIES patients. It is of note, however, that CGD patients suffer from staphylococcal infections that occur in a wide variety of organs, including the lung, lymph nodes, skin, liver, bone, gastrointestinal tract, kidney, and brain (33). The difference in the spectrum of affected tissues between HIES and CGD patients strongly suggests that the host factors, in addition to the pathogen's intrinsic factors, would determine the preferential sites of infections. In HIES patients, unlike in CGD patients, the neutrophils themselves are normal in their number and function; however, they probably cannot be recruited to the skin and lung because HIES T cells cannot induce the skin and lung epithelial cells to produce neutrophil-recruiting chemokines like CXCL8, even though we cannot formally exclude the possibility that the STAT3 mutation in the epithelial cells of HIES patients also contributes to impaired production of antistaphylococcal factors including CXCL8. Mice deficient for IL-17RA or IL-22 and mice treated with an anti–IL-17A blocking antibody are susceptible to infections with Gram-negative bacteria, such as *K. pneumoniae*, *M. pulmonis*, *B. fragilis*, *E. coli*, and *Citrobacter rodentium*, which are rarely observed in HIES patients (16, 17, 20, 21, 36, 37). The reason for this difference between human and mouse in bacterial susceptibility remains to be determined.

TLR-mediated signals are known to be important for immune protection from staphylococcal infections. The outer cell wall of *Staphylococcus aureus* is composed of exposed peptidoglycan and lipoteichoic acid, which are recognized by TLR2 (38–40). Mice deficient in TLR2 and patients deficient in IRAK4, a transducer of TLR signaling, show increased susceptibility to staphylococcal infections (41–43). Importantly, TLR2 signaling is intact in HIES patients (44, 45). We demonstrated in the present study that keratinocytes indeed produced antibacterial factors in response to TLR2 ligands, but the amounts were <10% of those induced when the cells were stimulated with the combination of Th17 and classical proinflammatory cytokines. Thus, TLR2-mediated signaling alone appears to be insufficient for the full protection against staphylococcal infection of the human skin and lung.

Skin and lung epithelial cells are located, respectively, at the major outer and inner surface barriers of the body, and are constantly exposed to agents from the environment. Therefore, these cells probably need to discriminate between infectious and noninfectious agents to avoid unnecessary inflammation. The present study demonstrated that they secrete antibacterial factors only when they receive stimuli from both classical proinflammatory cytokines delivered by innate immunity–type cells and Th17 cytokines delivered by T cells. Thus, an attractive hypothesis is that epithelial cells have been equipped by evolution to respond poorly to the first alert

Published June 1, 2009

signal, i.e., the classical proinflammatory cytokines produced by innate immunity cell types, which might be evoked even by noninfectious agents. Infectious agents, such as *S. aureus*, could evoke the production of the second alert signal, i.e., Th17 cytokines produced by T cells, in addition to the first alert signal. This would allow the epithelial cells to respond selectively to pathogens. In HIES patients, the second alert signal is not delivered because of the Th17 deficiency, which probably results in skin- and lung-restricted staphylococcal infections.

Accumulating evidence indicates that Th17 cells and their products are very important in the induction and propagation of autoimmunity (5–10). Therefore, the neutralization of Th17 cytokines appears to be a promising therapeutic strategy for the control of inflammation in autoimmune disorders. Moreover, antagonists of STAT3 are considered good candidates for the treatment of tumors because a variety of tumor cells show up-regulated STAT3 expression (46). However, our data indicate that such treatments would render patients susceptible to staphylococcal infection, particularly of the skin and lung, as observed in HIES. Fortunately, our study also suggests that this undesirable side effect might be prevented or treated by the local application of neutrophil-recruiting chemokines and BDs or their derivatives.

In summary, we demonstrated in the present study that T cells from HIES patients, in spite of their defect in production of Th17 cytokines, showed normal production of other proinflammatory cytokines including IL-1β in response to staphylococcal antigens, which was insufficient for triggering keratinocytes and bronchial epithelial cells but sufficient for other cell types to produce antistaphylococcal factors. This provides a possible molecular explanation for the apparent contradiction between the systemic Th17 deficiency and the skin- and lung-restricted staphylococcal infections in HIES patients.

MATERIALS AND METHODS

Patients. All eight patients enrolled in this study had typical findings associated with HIES and a National Institutes of Health score >40 points (27). The diagnosis was confirmed by the identification of the mutations in the *STAT3* gene. The study was approved by the Tokyo Medical and Dental University Ethics Committee, and written informed consent was obtained from the patients. All of the patients were in a healthy state when their blood samples were collected. Blood samples from patients and age-matched healthy subjects were obtained and PBMCs were prepared by density-gradient centrifugation.

Cell culture. PBMCs were cultured in 96-well plates in RPMI medium 1640 supplemented with 1% penicillin/streptomycin, 1% glutamine, and 10% heat-inactivated FCS. Cultures were stimulated with a 1:100 (vol/vol) dilution of anti-CD3 and anti-CD28 beads (Invitrogen). For some experiments, the following mAbs, cytokines, and TLR ligands were added: 20 ng/ml IL-17A, 200 ng/ml IL-17F, and 200 ng/ml IL-22 (R&D Systems); 10 ng/ml TNF-α, 10 ng/ml IL-1β, 10 ng/ml IFN-γ (PeproTech); neutralizing antibodies against IL-17, IL-22, and BD3 (R&D Systems); TLR ligands (InvivoGen); fixed *S. aureus* (EMD); SEB (Toxin Technology); and *C. albicans* skin test antigen (Torii Pharmaceutical Co., Ltd).

Culture of human keratinocytes, bronchial epithelial cells, fibroblasts, endothelial cells, and macrophages. Human epidermal keratinocytes and bronchial epithelial cells (Lonza) were propagated as adherent cells to plastic in RPMI 1640 medium containing bovine pituitary extract, human epidermal growth factor, insulin, hydrocortisone, gentamicin, and amphotericin at 37°C in a 5% CO_2 incubator. Human primary dermal fibroblasts, HUVEC, HMVEC-L were obtained from Lonza. Macrophages were derived from adherent cells in PBMCs cultured in the presence of 30 ng/ml GM-CSF for 7 d.

RNA isolation and real-time quantitative RT-PCR. Cells were harvested for total RNA isolation using the RNeasy Miniprep kit (QIAGEN), according to the manufacturer's instructions. Total RNA was reverse transcribed using the PrimeScript transcription kit (Takara Bio Inc.). An aliquot of the RT reaction was used as a template for real-time PCR in triplicate using a SYBR Green MasterMix (Takara Bio Inc.) on an Mx3005P thermocycler (Agilent Technologies) with SYBR green I dye as the amplicon detector and ROX as the passive reference. The gene for HPRT was amplified as an endogenous reference. Quantification was determined using both a standard curve and comparative ΔΔCT methods.

ELISA. Conditioned medium from cultured cells was collected after the cells were stimulated and stored at −80°C until use. IL-17A (eBioscience), IL-22 (R&D Systems), IFN-γ, TNF-α, IL-1β, CXCL8 (BD), BD2 (KOMABIOTECH), and BD3 (Alpha Diagnostics) were measured in triplicate by ELISA according to the manufacturers' instructions.

Bactericidal activity against *S. aureus*. *S. aureus* (strain Rosenbach 1884) was obtained from the National Biological Resource Center. Bactericidal activity was evaluated by plating serial dilutions of *S. aureus* mixed with the supernatant from keratinocytes or bronchial epithelial cells, and the CFUs were determined in triplicate on the next day. In some experiments, a neutralizing antibody to BD3 was added to the supernatant.

Chemotaxis. Chemotaxis of neutrophils was determined in triplicate by the Boyden chamber technique. The migration chamber was divided into upper and lower compartments by a membrane with a pore size of 3 μm. The neutrophils were placed into the upper compartment at a concentration of 10^6/ml, and the lower compartment contained the supernatant from the keratinocytes or fibroblasts grown under the conditions indicated. The chambers were incubated at 37° C for 1 h, and the number of neutrophils that migrated to the lower chamber was counted.

Immunoblotting. Cells were lysed on ice for 30 min in lysis buffer containing 1% Triton X-100, 50 mM Tris, pH 8.0, 150 mM NaCl, 2 mM EDTA, 2 μg/ml aprotinin, and 100 μg/ml PMSF. The cell lysates were subjected to SDS-PAGE, followed by electrotransfer to PVDF membranes and immunoblotting with antibodies for IL-1R1, IL-1R2, and IL-1Ra (R&D Systems) and for tubulin (Sigma-Aldrich).

Statistical analysis. Data were compared by a two-tailed Mann-Whitney *U* test or unpaired Student's *t* test. P-values < 0.05 were considered significant.

Online supplemental material. Fig. S1 shows the quantitative RT-PCR analysis for chemokine and BD expression in activated keratinocytes. The importance of IL-17A and IL-22 in stimulating keratinocytes to produce antistaphylococcal factors is demonstrated in Fig. S2. Fig. S3 shows the quantitative RT-PCR analysis for chemokine and BD expression in various types of cells. Production of CXCL8 by keratinocytes and fibroblasts in response to various cytokines is displayed in Figs. S4 and S5. Fig. S6 shows the expression and production of antistaphylococcal factors by keratinocytes in response to various stimuli. Up-regulation of the Th17 cytokine receptors in keratinocytes in response to classical inflammatory cytokines is displayed in Fig. S7. Online supplemental material is available at http://www.jem.org/cgi/content/full/jem.20082767/DC1.

This work is supported by Grants-in-Aid 16616004, 17047013, and 18659299 from the Japanese Ministry of Education, Culture, Sports, Science and Technology and Research on Intractable Diseases from the Ministry of Health, Labor and Welfare, the Uehara Foundation, Naito Foundation, and the Mother and Child Health Foundation.

The authors have no conflicting financial interests.

Published June 1, 2009

JEM

Submitted: 9 December 2008
Accepted: 14 May 2009

REFERENCES

1. Dong, C. 2008. TH17 cells in development: an updated view of their molecular identity and genetic programming. *Nat. Rev. Immunol.* 8:337–348.
2. Ivanov, I.I., L. Zhou, and D.R. Littman. 2007. Transcriptional regulation of Th17 cell differentiation. *Semin. Immunol.* 19:409–417.
3. Chen, Z., A. Laurence, and J.J. O'Shea. 2007. Signal transduction pathways and transcriptional regulation in the control of Th17 differentiation. *Semin. Immunol.* 19:400–408.
4. McGeachy, M.J., K.S. Bak-Jensen, Y. Chen, C.M. Tato, W. Blumenschein, T. McClanahan, and D.J. Cua. 2007. TGF-beta and IL-6 drive the production of IL-17 and IL-10 by T cells and restrain T(H)-17 cell-mediated pathology. *Nat. Immunol.* 8:1390–1397.
5. Cua, D.J., J. Sherlock, Y. Chen, C.A. Murphy, B. Joyce, B. Seymour, L. Lucian, W. To, S. Kwan, T. Churakova, et al. 2003. Interleukin-23 rather than interleukin-12 is the critical cytokine for autoimmune inflammation of the brain. *Nature.* 421:744–748.
6. Korn, T., M. Oukka, and E. Bettelli. 2007. Th17 cells: effector T cells with inflammatory properties. *Semin. Immunol.* 19:362–371.
7. Aujla, S.J., P.J. Dubin, and J.K. Kolls. 2007. Th17 cells and mucosal host defense. *Semin. Immunol.* 19:377–382.
8. Ouyang, W., J.K. Kolls, and Y. Zheng. 2008. The biological functions of T helper 17 cell effector cytokines in inflammation. *Immunity.* 28:454–467.
9. Diveu, C., M.J. McGeachy, and D.J. Cua. 2008. Cytokines that regulate autoimmunity. *Curr. Opin. Immunol.* 20:663–668.
10. Iwakura, Y., S. Nakae, S. Saijo, and H. Ishigame. 2008. The roles of IL-17A in inflammatory immune responses and host defense against pathogens. *Immunol. Rev.* 226:57–79.
11. Kolls, J.K., and A. Linden. 2004. Interleukin-17 family members and inflammation. *Immunity.* 21:467–476.
12. Kolls, J.K., P.B. McCray Jr., and Y.R. Chan. 2008. Cytokine-mediated regulation of antimicrobial proteins. *Nat. Rev. Immunol.* 8:829–835.
13. Kreymborg, K., R. Etzensperger, L. Dumoutier, S. Haak, A. Rebollo, T. Buch, F.L. Heppner, J.C. Renauld, and B. Becher. 2007. IL-22 is expressed by Th17 cells in an IL-23-dependent fashion, but not required for the development of autoimmune encephalomyelitis. *J. Immunol.* 179:8098–8104.
14. Wolk, K., S. Kunz, E. Witte, M. Friedrich, K. Asadullah, and R. Sabat. 2004. IL-22 increases the innate immunity of tissues. *Immunity.* 21:241–254.
15. Toy, D., D. Kugler, M. Wolfson, T. Vanden Bos, J. Gurgel, J. Derry, J. Tocker, and J. Peschon. 2006. Cutting edge: interleukin 17 signals through a heteromeric receptor complex. *J. Immunol.* 177:36–39.
16. Aujla, S.J., Y.R. Chan, M. Zheng, M. Fei, D.J. Askew, D.A. Pociask, T.A. Reinhart, F. McAllister, J. Edeal, K. Gaus, et al. 2008. IL-22 mediates mucosal host defense against Gram-negative bacterial pneumonia. *Nat. Med.* 14:275–281.
17. Zheng, Y., P.A. Valdez, D.M. Danilenko, Y. Hu, S.M. Sa, Q. Gong, A.R. Abbas, Z. Modrusan, N. Ghilardi, F.J. de Sauvage, and W. Ouyang. 2008. Interleukin-22 mediates early host defense against attaching and effacing bacterial pathogens. *Nat. Med.* 14:282–289.
18. Ishigame, H., S. Kakuta, T. Nagai, M. Kadoki, A. Nambu, Y. Komiyama, N. Fujikado, Y. Tanahashi, A. Akitsu, H. Kotaki, et al. 2009. Differential roles of interleukin-17A and -17F in host defense against mucoepithelial bacterial infection and allergic responses. *Immunity.* 30:108–119.
19. Higgins, S.C., A.G. Jarnicki, E.C. Lavelle, and K.H. Mills. 2006. TLR4 mediates vaccine-induced protective cellular immunity to *Bordetella pertussis*: role of IL-17-producing T cells. *J. Immunol.* 177:7980–7989.
20. Chung, D.R., D.L. Kasper, R.J. Panzo, T. Chitnis, M.J. Grusby, M.H. Sayegh, and A.O. Tzianabos. 2003. CD4+ T cells mediate abscess formation in intra-abdominal sepsis by an IL-17-dependent mechanism. *J. Immunol.* 170:1958–1963.
21. Shibata, K., H. Yamada, H. Hara, K. Kishihara, and Y. Yoshikai. 2007. Resident Vdelta1+ gammadelta T cells control early infiltration of neutrophils after *Escherichia coli* infection via IL-17 production. *J. Immunol.* 178:4466–4472.
22. Huang, W., L. Na, P.L. Fidel, and P. Schwarzenberger. 2004. Requirement of interleukin-17A for systemic anti-*Candida albicans* host defense in mice. *J. Infect. Dis.* 190:624–631.
23. Milner, J.D., J.M. Brenchley, A. Laurence, A.F. Freeman, B.J. Hill, K.M. Elias, Y. Kanno, C. Spalding, H.Z. Elloumi, M.L. Paulson, et al. 2008. Impaired T(H)17 cell differentiation in subjects with autosomal dominant hyper-IgE syndrome. *Nature.* 452:773–776.
24. Ma, C.S., G.Y. Chew, N. Simpson, A. Priyadarshi, M. Wong, B. Grimbacher, D.A. Fulcher, S.G. Tangye, and M.C. Cook. 2008. Deficiency of Th17 cells in hyper IgE syndrome due to mutations in *STAT3*. *J. Exp. Med.* 205:1551–1557.
25. de Beaucoudrey, L., A. Puel, O. Filipe-Santos, A. Cobat, P. Ghandil, M. Chrabieh, J. Feinberg, H. von Bernuth, A. Samarina, L. Janniere, et al. 2008. Mutations in *STAT3* and *IL12RB1* impair the development of human IL-17–producing T cells. *J. Exp. Med.* 205:1543–1550.
26. Renner, E.D., S. Rylaarsdam, S. Anover-Sombke, A.L. Rack, J. Reichenbach, J.C. Carey, Q. Zhu, A.F. Jansson, J. Barboza, L.F. Schimke, et al. 2008. Novel signal transducer and activator of transcription 3 (STAT3) mutations, reduced T(H)17 cell numbers, and variably defective STAT3 phosphorylation in hyper-IgE syndrome. *J. Allergy Clin. Immunol.* 122:181–187.
27. Minegishi, Y., M. Saito, S. Tsuchiya, I. Tsuge, H. Takada, T. Hara, N. Kawamura, T. Ariga, S. Pasic, O. Stojkovic, et al. 2007. Dominant-negative mutations in the DNA-binding domain of STAT3 cause hyper-IgE syndrome. *Nature.* 448:1058–1062.
28. Holland, S.M., F.R. DeLeo, H.Z. Elloumi, A.P. Hsu, G. Uzel, N. Brodsky, A.F. Freeman, A. Demidowich, J. Davis, M.L. Turner, et al. 2007. STAT3 mutations in the hyper-IgE syndrome. *N. Engl. J. Med.* 357:1608–1619.
29. Grimbacher, B., S.M. Holland, and J.M. Puck. 2005. Hyper-IgE syndromes. *Immunol. Rev.* 203:244–250.
30. Minegishi, Y., and H. Karasuyama. 2007. Hyperimmunoglobulin E syndrome and tyrosine kinase 2 deficiency. *Curr. Opin. Allergy Clin. Immunol.* 7:506–509.
31. Minegishi, Y., and H. Karasuyama. 2008. Genetic origins of hyper-IgE syndrome. *Curr. Allergy Asthma Rep.* 8:386–391.
32. Minegishi, Y., and H. Karasuyama. 2009. Defects in Jak-STAT-mediated cytokine signals cause hyper-IgE syndrome: lessons from a primary immunodeficiency. *Int. Immunol.* 21:105–112.
33. Winkelstein, J.A., M.C. Marino, R.B. Johnston Jr., J. Boyle, J. Curnutte, J.I. Gallin, H.L. Malech, S.M. Holland, H. Ochs, P. Quie, et al. 2000. Chronic granulomatous disease. Report on a national registry of 368 patients. *Medicine (Baltimore).* 79:155–169.
34. Sumikawa, Y., H. Asada, K. Hoshino, H. Azukizawa, I. Katayama, S. Akira, and S. Itami. 2006. Induction of beta-defensin 3 in keratinocytes stimulated by bacterial lipopeptides through toll-like receptor 2. *Microbes Infect.* 8:1513–1521.
35. Pivarcsi, A., L. Bodai, B. Rethi, A. Kenderessy-Szabo, A. Koreck, M. Szell, Z. Beer, Z. Bata-Csorgoo, M. Magocsi, E. Rajnavolgyi, et al. 2003. Expression and function of Toll-like receptors 2 and 4 in human keratinocytes. *Int. Immunol.* 15:721–730.
36. Happel, K.I., P.J. Dubin, M. Zheng, N. Ghilardi, C. Lockhart, L.J. Quinton, A.R. Odden, J.E. Shellito, G.J. Bagby, S. Nelson, and J.K. Kolls. 2005. Divergent roles of IL-23 and IL-12 in host defense against *Klebsiella pneumoniae*. *J. Exp. Med.* 202:761–769.
37. Tan, W., W. Huang, Q. Zhong, and P. Schwarzenberger. 2006. IL-17 receptor knockout mice have enhanced myelotoxicity and impaired hemopoietic recovery following gamma irradiation. *J. Immunol.* 176:6186–6193.
38. Yoshimura, A., E. Lien, R.R. Ingalls, E. Tuomanen, R. Dziarski, and D. Golenbock. 1999. Cutting edge: recognition of Gram-positive bacterial cell wall components by the innate immune system occurs via Toll-like receptor 2. *J. Immunol.* 163:1–5.
39. Lien, E., T.J. Sellati, A. Yoshimura, T.H. Flo, G. Rawadi, R.W. Finberg, J.D. Carroll, T. Espevik, R.R. Ingalls, J.D. Radolf, and D.T. Golenbock. 1999. Toll-like receptor 2 functions as a pattern recognition receptor for diverse bacterial products. *J. Biol. Chem.* 274:33419–33425.
40. Schwandner, R., R. Dziarski, H. Wesche, M. Rothe, and C.J. Kirschning. 1999. Peptidoglycan- and lipoteichoic acid-induced cell activation is mediated by toll-like receptor 2. *J. Biol. Chem.* 274:17406–17409.

41. Takeuchi, O., K. Hoshino, T. Kawai, H. Sanjo, H. Takada, T. Ogawa, K. Takeda, and S. Akira. 1999. Differential roles of TLR2 and TLR4 in recognition of gram-negative and gram-positive bacterial cell wall components. *Immunity.* 11:443–451.
42. Takeuchi, O., K. Hoshino, and S. Akira. 2000. Cutting edge: TLR2-deficient and MyD88-deficient mice are highly susceptible to *Staphylococcus aureus* infection. *J. Immunol.* 165:5392–5396.
43. Ku, C.L., H. von Bernuth, C. Picard, S.Y. Zhang, H.H. Chang, K. Yang, M. Chrabieh, A.C. Issekutz, C.K. Cunningham, J. Gallin, et al. 2007. Selective predisposition to bacterial infections in IRAK-4–deficient children: IRAK-4–dependent TLRs are otherwise redundant in protective immunity. *J. Exp. Med.* 204:2407–2422.
44. Hawn, T.R., A. Ozinsky, L.M. Williams, S. Rodrigues, A. Clark, U. Pham, H.R. Hill, H. Ochs, A. Aderem, and W.C. Liles. 2005. Hyper-IgE syndrome is not associated with defects in several candidate toll-like receptor pathway genes. *Hum. Immunol.* 66:842–847.
45. Renner, E.D., I. Pawlita, F. Hoffmann, V. Hornung, D. Hartl, M. Albert, A. Jansson, S. Endres, G. Hartmann, B.H. Belohradsky, and S. Rothenfusser. 2005. No indication for a defect in toll-like receptor signaling in patients with hyper-IgE syndrome. *J. Clin. Immunol.* 25:321–328.
46. Yu, H., M. Kortylewski, and D. Pardoll. 2007. Crosstalk between cancer and immune cells: role of STAT3 in the tumour microenvironment. *Nat. Rev. Immunol.* 7:41–51.

Immunity
Resource

Functional Delineation and Differentiation Dynamics of Human CD4$^+$ T Cells Expressing the FoxP3 Transcription Factor

Makoto Miyara,[1,10] Yumiko Yoshioka,[1,9] Akihiko Kitoh,[1,9] Tomoko Shima,[1,9] Kajsa Wing,[1] Akira Niwa,[2] Christophe Parizot,[3] Cécile Taflin,[3] Toshio Heike,[2] Dominique Valeyre,[4] Alexis Mathian,[3] Tatsutoshi Nakahata,[2] Tomoyuki Yamaguchi,[1] Takashi Nomura,[1] Masahiro Ono,[1] Zahir Amoura,[5,6] Guy Gorochov,[3,6] and Shimon Sakaguchi[1,7,8,*]

[1]Department of Experimental Pathology, Institute for Frontier Medical Sciences
[2]Department of Pediatrics, Graduate School of Medicine
Kyoto University, Kyoto 606-8507, Japan
[3]Institut National de la Santé et de la Recherche Médicale (INSERM) UMR-S 945, Laboratoire AP-HP d'immunologie cellulaire et tissulaire, Hôpital Pitié-Salpêtrière, 75013 Paris, France
[4]Pneumology Department, AP-HP Hôpital Avicenne, 93000 Bobigny, France
[5]Internal Medicine Department, AP-HP Hôpital Pitié-Salpêtrière, 75013 Paris, France
[6]Pierre and Marie Curie University, UPMC Paris Universitas, 75005 Paris, France
[7]Core Research for Evolutional Science and Technology (CREST), Japan Science and Technology Agency, Kawaguchi 332-0012, Japan
[8]WPI Immunology Frontier Research Center, Osaka University, Suita 565-0871, Japan
[9]These authors contributed equally to this work
[10]Present address: Internal Medicine Department and Institut National de la Santé et de la Recherche Médicale (INSERM) UMR-S 945, Laboratoire AP-HP d'immunologie cellulaire et tissulaire, Hôpital Pitié-Salpêtrière, 75013 Paris, France
*Correspondence: shimon@frontier.kyoto-u.ac.jp
DOI 10.1016/j.immuni.2009.03.019

SUMMARY

FoxP3 is a key transcription factor for the development and function of natural CD4$^+$ regulatory T cells (Treg cells). Here we show that human FoxP3$^+$CD4$^+$ T cells were composed of three phenotypically and functionally distinct subpopulations: CD45RA$^+$FoxP3^{lo} resting Treg cells (rTreg cells) and CD45RA$^-$FoxP3^{hi} activated Treg cells (aTreg cells), both of which were suppressive in vitro, and cytokine-secreting CD45RA$^-$FoxP3^{lo} nonsuppressive T cells. The proportion of the three subpopulations differed between cord blood, aged individuals, and patients with immunological diseases. Terminally differentiated aTreg cells rapidly died whereas rTreg cells proliferated and converted into aTreg cells in vitro and in vivo. This was shown by the transfer of rTreg cells into NOD-scid-common γ-chain-deficient mice and by TCR sequence-based T cell clonotype tracing in peripheral blood in a normal individual. Taken together, the dissection of FoxP3$^+$ cells into subsets enables one to analyze Treg cell differentiation dynamics and interactions in normal and disease states, and to control immune responses through manipulating particular FoxP3$^+$ subpopulations.

INTRODUCTION

FoxP3-expressing CD4$^+$ thymus-derived naturally occurring regulatory T cells (Treg cells) play an indispensable role for the maintenance of self tolerance and immune homeostasis (Sakaguchi et al., 2008). They play crucial roles in human diseases, such as autoimmune disease, allergy, and cancer (Curiel et al., 2004; Ehrenstein et al., 2004; Kriegel et al., 2004; Miyara et al., 2005; Viglietta et al., 2004). Human natural Treg cells were initially defined according to their high expression of CD25 (Baecher-Allan et al., 2001; Dieckmann et al., 2001; Jonuleit et al., 2001; Levings et al., 2001; Ng et al., 2001; Taams et al., 2001), based on the finding that murine CD25$^+$CD4$^+$ T cells are highly suppressive (Sakaguchi et al., 1995). With the discovery of FoxP3 as a "master control gene" for CD4$^+$ Treg cell development and function (Fontenot et al., 2003; Hori et al., 2003; Khattri et al., 2003), detection of FoxP3 at the mRNA and protein level revealed that human CD25^{hi}CD4$^+$ T cells indeed express FoxP3 (Miyara et al., 2006; Roncador et al., 2005; Yagi et al., 2004). In contrast to murine FoxP3$^+$ Treg cells, however, human FoxP3$^+$ cells may not be functionally homogenous. For example, it has been reported that mere TCR stimulation can induce FoxP3 expression in apparently naive human FoxP3$^-$CD4$^+$ T cells without conferring suppressive activity (Allan et al., 2007; Gavin et al., 2006; Tran et al., 2007; Wang et al., 2007). Furthermore, some FoxP3$^+$ cells are phenotypically naive (e.g., CD45RA$^+$), present in cord blood as well as in peripheral blood of adults, and suppressive in vitro (Valmori et al., 2005), whereas other FoxP3$^+$ cells phenotypically resemble memory T cells (e.g., CD45RA$^-$) and are suggested to originate from peripheral memory FoxP3$^-$CD4$^+$ T cells (Vukmanovic-Stejic et al., 2006). To better understand the roles of FoxP3$^+$ T cells for the control of immune responses, it is necessary to determine whether FoxP3-expressing T cells in freshly isolated CD4$^+$ T cells are functionally heterogeneous, how functionally different subpopulations of FoxP3$^+$ cells can be reliably delineated, and how such

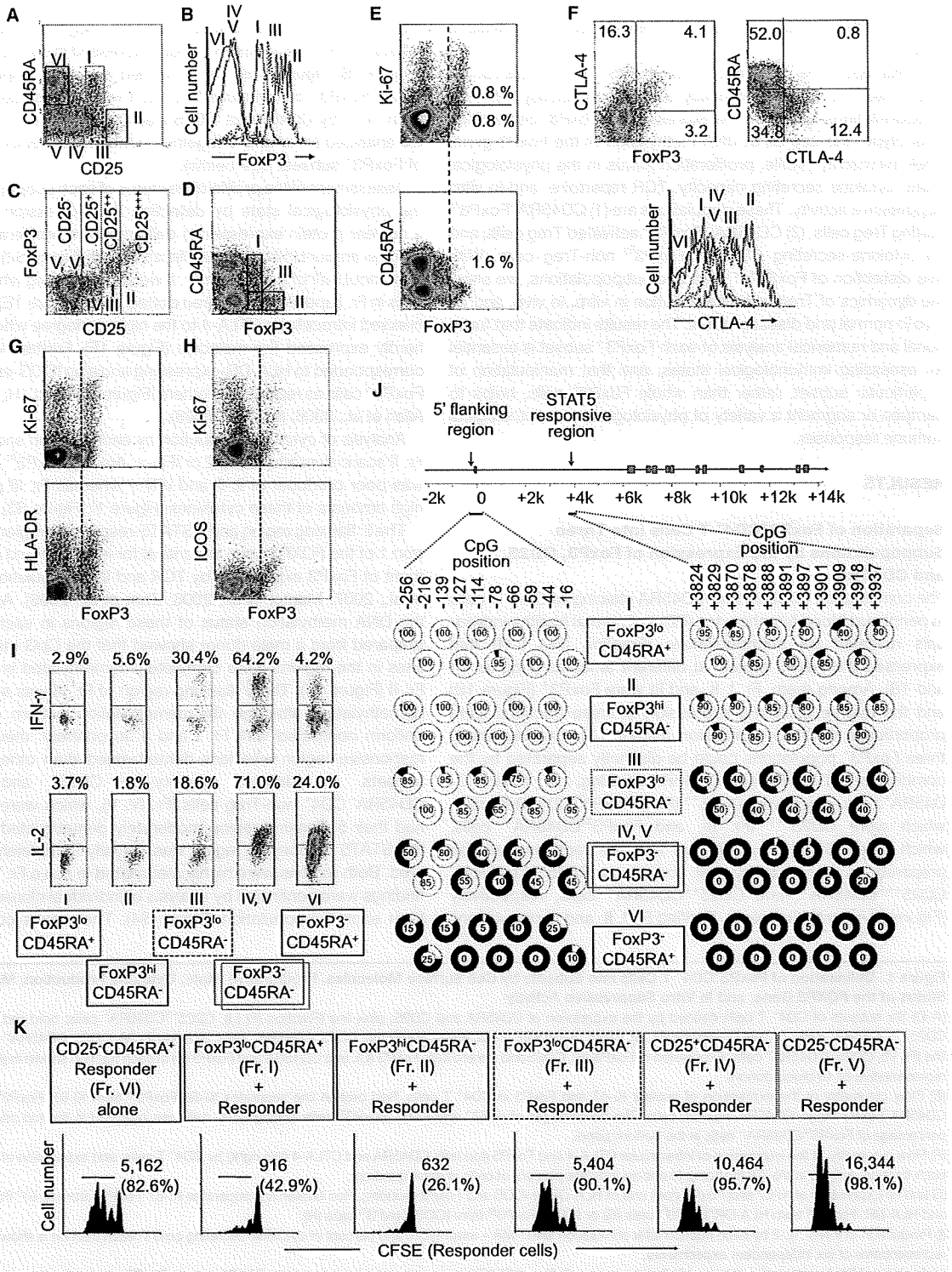
A
CD45RA
CD25
B
Cell number
FoxP3
C
FoxP3
CD25
D
CD45RA
FoxP3
E
Ki-67
0.8 %
0.8 %
CD45RA
1.6 %
FoxP3
F
CTLA-4
16.3
4.1
3.2
FoxP3
CD45RA
52.0
0.8
34.6
12.4
CTLA-4
Cell number
CTLA-4
G
Ki-67
HLA-DR
FoxP3
H
Ki-67
ICOS
FoxP3
I
IFN-γ
2.9%
5.6%
30.4%
64.2%
4.2%
IL-2
3.7%
1.8%
18.6%
71.0%
24.0%
FoxP3lo CD45RA+
FoxP3hi CD45RA-
FoxP3lo CD45RA-
FoxP3- CD45RA-
FoxP3- CD45RA+
J
5' flanking region
STAT5 responsive region
-2k 0 +2k +4k +6k +8k +10k +12k +14k
CpG position
CpG position
FoxP3lo CD45RA+
FoxP3hi CD45RA-
FoxP3lo CD45RA-
FoxP3- CD45RA-
FoxP3- CD45RA+
K
CD25-CD45RA+ Responder (Fr. VI) alone
FoxP3loCD45RA+ (Fr. I) + Responder
FoxP3hiCD45RA- (Fr. II) + Responder
FoxP3loCD45RA- (Fr. III) + Responder
CD25+CD45RA- (Fr. IV) + Responder
CD25-CD45RA- (Fr. V) + Responder
Cell number
5,162 (82.6%)
916 (42.9%)
632 (26.1%)
5,404 (90.1%)
10,464 (95.7%)
16,344 (98.1%)
CFSE (Responder cells)

subsets differentiate and interact in physiological and disease states.

In this report, we show that human FoxP3$^+$CD4$^+$ T cells can be separated into three functionally and phenotypically different subpopulations based on the expression of FoxP3, cell surface phenotype, the degree of DNA methylation of the FoxP3 gene, DNA microarray profile, proliferation status in the physiological state, cytokine secreting capacity, TCR repertoire, and in vitro suppressive activity. These populations are (1) CD45RA$^+$FoxP3^{lo} resting Treg cells, (2) CD45RA$^-$FoxP3^{hi} activated Treg cells, and (3) cytokine-secreting CD45RA$^-$FoxP3^{lo} non-Treg cells. With this dissection of FoxP3$^+$ T cells into subpopulations, we show the dynamics of Treg cell differentiation in vitro, in vivo, and ex vivo in normal and disease states. The results indicate that functional and numerical analysis of each FoxP3$^+$ subset is essential for assessing immunological states, and that manipulation of a particular subset, rather than whole FoxP3$^+$ cells, helps to dampen or augment a variety of physiological and pathological immune responses.

RESULTS

Separation of FoxP3$^+$CD4$^+$ T Cells into Three Subpopulations by the Expression of FoxP3, CD25, and CD45RA

The combination of CD25 and CD45RA staining of CD4$^+$ T cells in peripheral blood lymphocytes (PBL) of normal healthy individuals revealed six subpopulations (Fraction [Fr.] I–VI) that expressed the FoxP3 protein at different amounts (Figures 1A and 1B). Among them, Fr. I, II, and III were FoxP3$^+$ (Figure 1B) and the degree of FoxP3 expression in these fractions were proportional to CD25 expression (Figure 1C). Notably, these three FoxP3$^+$ populations could be distinctly separated by the combination of FoxP3 and CD45RA staining; i.e., FoxP3^{lo}CD45RA$^+$ cells, which were CD25^{++} (Fr. I), FoxP3^{hi}CD45RA$^-$ cells, which were CD25^{+++} (Fr. II), and FoxP3^{lo}CD45RA$^-$ cells, which were CD25^{++} (Fr. III) (Figure 1D). The fractions could be prepared as live cells by cell sorting as CD25^{++}CD45RA$^+$, CD25^{+++}CD45RA$^-$, and CD25^{++}CD45RA$^-$ cells, respectively (Figure S1A available online). Purified Fr. I, II, and III populations expressed FoxP3 transcripts to a similar degree irrespective of different amounts of FoxP3 protein expressed in each population (Figure 1B; Figure S1B). Fr. IV formed a distinct population as CD25$^+$FoxP3$^-$ cells (Figure 1C), but it was not well demarcated from Fr. V by CD45RA or CD25 staining (Figure 1A). Therefore, we analyzed Fr. IV and V together in the functional examination of FoxP3$^+$ subsets (see below).

Assessment of the proliferative status of each subpopulation in the physiological state by detecting the expression of Ki-67, a nuclear protein expressed in cells ready to proliferate and at a higher amount in actually proliferating cells (Figure S2), revealed that about half of the cells in Fr. II were proliferating whereas the cells in Fr. I and III were not (red dotted line in Figure 1E). Fr. II expressed intracellular CTLA-4 to the highest degree whereas Fr. I hardly expressed the molecule (Figure 1F). Furthermore, Fr. II corresponded to HLA-DR-expressing and also ICOS-expressing FoxP3$^+$ cells as reported by others (Figures 1G and 1H; Baecher-Allan et al., 2006; Ito et al., 2008).

Analysis of cytokine production by each fraction showed that Fr. II scarcely produced IL-2 or IFN-γ. Among FoxP3^{lo} cells, Fr. I was poor producer of IL-2 and IFN-γ whereas Fr. III produced high amounts of these cytokines (Figure 1I; Figure S3).

The5′ flanking region and a STAT5-responsive region in the intron 1 of the *FOXP3* gene are critical for induction and enhancement of FoxP3 expression by TCR and IL-2 stimulation (Floess et al., 2007; Mantel et al., 2006; Zorn et al., 2006). Analysis of the DNA methylation status of these regions in each fraction prepared from a male donor showed that the CpG methylation sites in the regions were completely demethylated in Fr. I and Fr. II (Figure 1J). The 5′ flanking region of Fr. III was also highly demethylated, although the demethylation pattern was less uniform compared with Fr. I and II. In contrast, their STAT5-responsive region was less demethylated than other FoxP3$^+$ subsets. In addition, memory-like CD25$^+$ and CD25$^-$ CD45RA$^-$CD4$^+$ non-Treg cells (Fr. IV, V), which were FoxP3$^-$, had their 5′ flanking region moderately demethylated whereas the STAT5 responsive region was virtually completely methylated. Both regions were highly methylated in naive Fr. VI. These findings were confirmed by analysis of individual clones isolated from each subpopulation (Figure S4). The results collectively

Figure 1. Delineation of FoxP3$^+$CD4$^+$ T Cells into Subsets by Cell Surface Molecules, Proliferative State, Cytokine Production, Methylation Status of the *FOXP3* Gene, and In Vitro Suppressive Activity

(A–D) Six subsets of CD4$^+$ T cells defined by the expression of CD45RA and CD25: pink line (Fraction [Fr.] I), CD25^{++}CD45RA$^+$ cells; bold red line (Fr. II), CD25^{+++}CD45RA$^-$ cells; broken brown line (Fr. III), CD25^{++}CD45RA$^-$ cells; green line (Fr. IV), CD25$^+$CD45RA$^-$ cells; blue line (Fr. V), CD25$^-$CD45RA$^-$ cells; black line (Fr. VI), CD25$^-$CD45RA$^+$ cells. Expression of FoxP3 (B), CD25 and intracellular FoxP3 (C), and CD45RA and FoxP3 (D) in each fraction shown in (A). Data are representative of 19 blood donors.

(E) Flow cytometry of the expression of nuclear Ki-67 and FoxP3 in CD4$^+$ T cells. Red broken line separates Ki-67$^+$FoxP3^{hi} from Ki-67$^-$FoxP3^{lo} cells and CD45RA$^+$FoxP3^{lo} from CD45RA$^-$FoxP3^{hi} cells. The percentages of Ki-67$^+$ and Ki-67$^-$FoxP3^{hi} cells among CD4$^+$ cells are indicated in the top panel and the percentage of FoxP3^{hi}CD45RA$^-$ cells in the bottom panel.

(F) Flow cytometry of the expression of intracellular CTLA-4 and FoxP3 (top left); CD45RA and CTLA-4 (top right) by CD4$^+$ T cells; and expression of CTLA-4 by each fraction defined in (A)–(D) (bottom). Numbers indicate percent of cells in each quadrant.

(G and H) Expression of Ki-67 and FoxP3 (top) and of HLA-DR or ICOS and FoxP3 (bottom). Red broken line separates Ki-67$^+$FoxP3^{hi} from Ki-67$^-$FoxP3^{lo} cells and HLA-DR$^-$FoxP3^{lo} from HLA-DR$^+$FoxP3^{hi} cells (G) or ICOS$^-$FoxP3^{lo} from ICOS$^+$FoxP3^{hi} cells (H).

(I) Production of IFN-γ, IL-2 by each fraction after stimulation with PMA + ionomycin, and percent of cytokine-secreting cells in each fraction is shown. Data are representative of six independent experiments.

(J) Analysis of DNA methylation status at 5′ flanking region (left) and STAT5-responsive (right) region of the *FOXP3* gene in FoxP3-expressing or -nonexpressing CD4$^+$ T cell subsets (Figure S1) from PBMCs of one healthy male donor. Percentages of clones displaying demethylation of indicated CpG methylation sites are indicated and depicted in white in sector graphs. 19 to 20 clones were sequenced from each CD4$^+$ T cell subset.

(K) CFSE dilution by 10^4 labeled CD25$^-$CD45RA$^+$CD4$^+$ responder T cells assessed after 84–90 hr of TCR-stimulated coculture with indicated CD4$^+$ T cell subset at a 1 to 1 ratio. Cell number and percentage of dividing cells per well are indicated. Data are representative of 12 separate experiments.

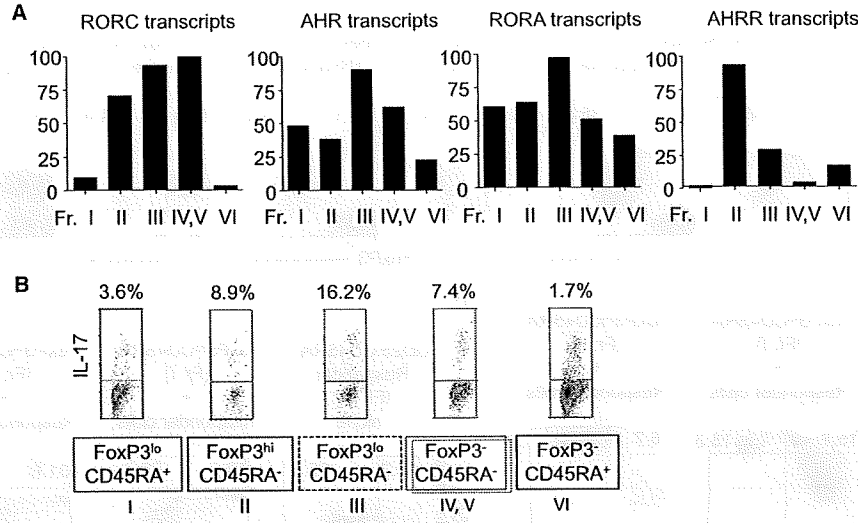

Figure 2. CD45RA$^-$FoxP3^{lo}CD4$^+$ T Cells Contain Cells with Th17 Cell Potential
(A) The amounts of transcripts of indicated genes in separated CD4$^+$ T cell subsets were assessed by quantitative PCR.
(B) Flow cytometry of the production of IL-17 by gated CD4$^+$ T cell subsets after stimulation with PMA + ionomycin for 5 hr. Percentages of cytokine-secreting cells are shown. Data are representative of six independent experiments.

indicate that Fr. I and II are active in FoxP3 gene transcription and close in their differentiation stage, and that, compared with these fractions, Fr. III may be less capable of maintaining FoxP3 expression in the presence of IL-2 and STAT5 signaling.

To assess the in vitro suppressive potency of each fraction, we measured the extent of CFSE dilution of labeled naive CD25$^-$CD45RA$^+$CD4$^+$ T cells (hereafter called responder cells) cocultured with an equal number of each fraction and stimulated for 4 days (Figure 1K). Fr. I and II (isolated as CD25^{++}CD45RA$^+$ and CD25^{+++}CD45RA$^-$ cells, respectively, as shown in Figure S1) potently suppressed the proliferation of responder cells, whereas Fr. III, IV, and V did not and even enhanced the responder proliferation. The inability of Fr. III (CD45RA$^-$Foxp3^{lo} cells) to suppress was confirmed by using CD127 as an additional marker for purifying FoxP3-expressing cells from CD4$^+$ T cells (Figure S5; Liu et al., 2006; Seddiki et al., 2006).

Taken together, three distinct subpopulations of FoxP3$^+$CD4$^+$ T cells can be defined in human PBL by the expression of CD45RA and FoxP3 as summarized in Table S1; i.e., Fr. I: CTLA-4^{lo}Ki-67$^-$CD45RA$^+$FoxP3^{lo} T cells; Fr. II: CTLA-4^{hi}CD45RA$^-$FoxP3^{hi} cells, both of which possess a fully functional *FOXP3* gene, hardly secrete cytokines, and potently suppress proliferation; and Fr. III: CTLA-4^{int}CD45RA$^-$FoxP3^{lo} T cells, which secrete cytokines, are much less active in the expression of the *FOXP3* gene under the control via STAT5, and do not suppress proliferation in vitro. Based on their phenotypic and functional characteristics, Fr. I and Fr. II can be designated as resting Treg cells (rTreg cells) and activated Treg cells (aTreg cells), respectively.

FoxP3^{lo}CD45RA$^-$ Nonregulatory T Cells Contain Cells with Th17 Cell Potential

DNA microarray analysis of each fraction showed that the gene expression patterns in the three FoxP3-expressing subpopulations were distinct (Figure S6A). Quantitative assessment of mRNA expression of differentially expressed genes revealed that the expression of RORC, a key transcription factor in Th17 cell lineage (Ivanov et al., 2006), was highly upregulated in Fr. II and III, indicating that RORC-FoxP3 double-positive population, which was recently described in mice (Yang et al., 2008a; Zhou et al., 2008), exists in humans as well in Fr. II and III (Figure S6B). Transcripts encoding RORα and AHR, both of which contribute to Th17 cell differentiation in mice (Veldhoen et al., 2008; Yang et al., 2008b), were highly upregulated in Fr.III, further indicating that this population contains cells with Th17 cell potential (Figure 2A). Also of note is that Fr. II specifically expressed high amounts of AHR repressor transcripts, suggesting that Treg cell differentiation might accompany an inhibition of Th17 cell differentiation via expression of AHR repressor. Assessment of cytokine production revealed that Fr. III was the highest producer of IL-17 even compared with naive FoxP3$^-$CD45RA$^+$ (Fr. VI) or memory-like FoxP3$^-$CD45RA$^-$CD4$^+$ non-Treg cells (Fr. IV and V) (Figure 2B; Figure S3).

Thus, DNA microarray profiling of FoxP3$^+$ subpopulations supports the relevance of separating FoxP3$^+$CD4$^+$ T cells into three subsets. Further, regarding the cell lineage relationship of FoxP3$^+$ cells and Th17 cells, Fr. III contains FoxP3-RORγ double-positive cells with a Th17 cell potential, in addition to IL-2- and/or IFN-γ-producing cells (Figure 1I).

Resting Treg Cells Proliferate whereas Activated Treg Cells Die while Suppressing In Vitro

As shown in Figure 1E, fresh Fr. I cells (rTreg cells) did not express Ki-67. However, when they were cocultured with responder cells and TCR stimulated, all the FoxP3-expressing cells became Ki-67$^+$ on day 4, indicating that rTreg cells proliferate (Figure S7). Assessment of proliferation by CFSE dilution during 4 days of culture also revealed that both aTreg cells

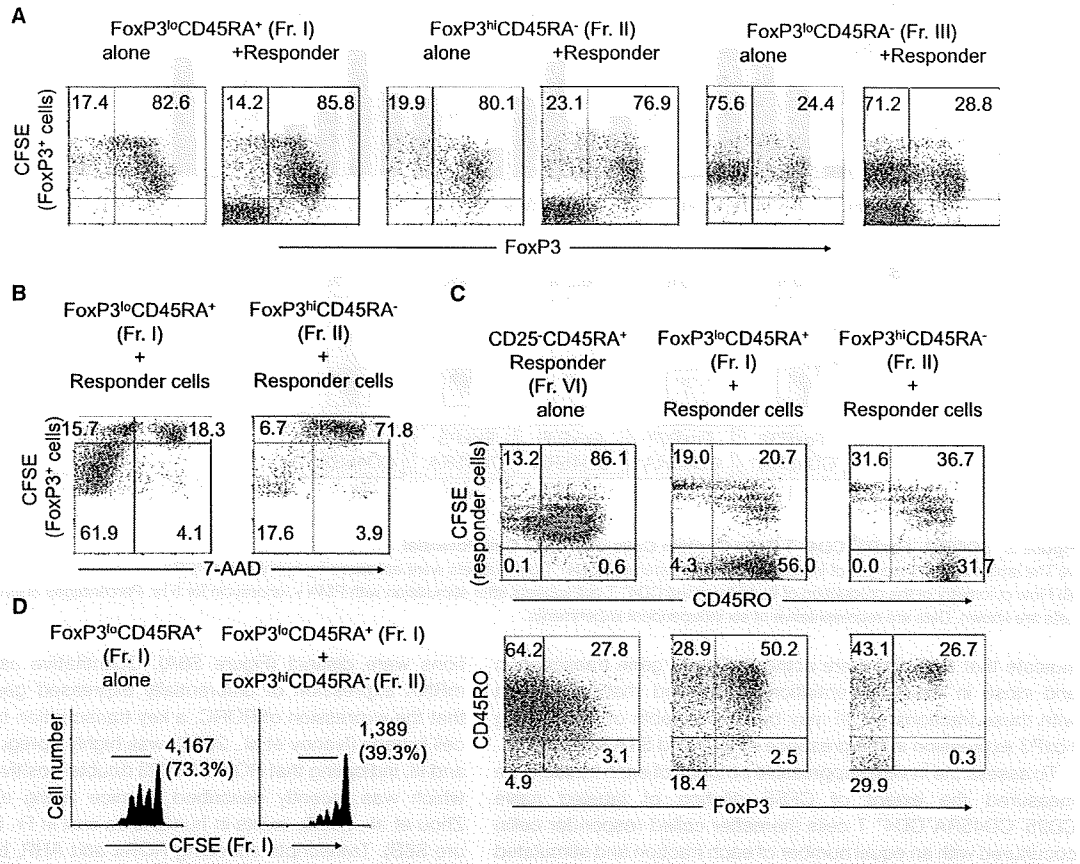

Figure 3. In Vitro Properties of FoxP3+ Subpopulations

(A) CFSE dilution by rTreg or aTreg cells and intracellular expression of FoxP3 were analyzed after 4 days TCR stimulation in the absence or presence of nonlabeled responder cells. Percentages of FoxP3− and of FoxP3+ cells among CFSE-labeled cells are indicated.

(B) Viability assessed by 7-AAD staining of CFSE-labeled CD45RA+FoxP3lo (left) or CD45RA−FoxP3hi Treg cells (right) cocultured with nonlabeled responder cells for 4 days. Only CFSE-labeled cells are shown. Numbers indicate percentage in each quadrant. Data shown are representative of five independent experiments.

(C) CFSE dilution, surface CD45RO, and intracellular FoxP3 expression by CFSE-labeled responder cells cultured alone or cocultured with unlabeled Treg cell subsets for 4 days. Numbers indicate percentage in each quadrant.

(D) CFSE dilution of labeled rTreg cells cultured alone or with aTreg cells at a 1 to 1 ratio. Numbers and percentage of proliferating cells are indicated. Data shown in (B) and (D) are representative of five independent experiments.

(Fr. II) and rTreg cells (Fr. I) gave rise to CFSE-diluting FoxP3+ cells when cultured alone (Figure 3A). In addition, rTreg cells showed more active proliferation than did aTreg cells in the presence of responder cells. In contrast with rTreg or aTreg cells, most (~70%) of CD45RA−FoxP3loCD4+ T cells (Fr. III) did not express FoxP3 during their proliferation, indicating that FoxP3 expression in the majority of Fr. III cells may not be stable in concordance with the methylation status of their *FOXP3* gene (Figure 3A).

Based on the finding that very few aTreg cells (Fr. II) were detectable after 4 days of culture (Figure S7), we assessed the viability of Treg cells by measuring incorporation of 7-AAD by CFSE-labeled rTreg or aTreg cells cultured with responder cells (Figure 3B). The majority (~75%) of aTreg cells were positive for 7-AAD. By contrast, although a fraction (~20%) of rTreg cells were nonproliferative and 7-AAD+, the majority of proliferating rTreg cells (~60%) were 7-AAD− (Figure 3B). In addition to proliferation, rTreg cells showed increased expression of FoxP3 (Figure 3A), CD45RO (Figure 3C), and intracellular CTLA-4 (Figure S8). High expression of CD45RO was secondary to activation because rTreg cells, which were CD45RA+, did not express CD45RO when freshly isolated from peripheral blood (Figure S9). Further, when CFSE-labeled rTreg cells (Fr. I) were cultured with nonlabeled aTreg cells (Fr. II), the latter substantially suppressed the proliferation of the former (Figure 3D).

Taken together, rTreg cells are not anergic and are able to proliferate upon TCR stimulation. They acquire a Ki-67+FoxP3hi aTreg cell phenotype and exert suppression during and after their proliferation and conversion to aTreg cells, which die after proliferation and exertion of suppression. Activated Treg cells also suppress the proliferation of resting Treg cells in a negative feedback fashion. Thus, in addition to different cell surface phenotypes, rTreg and aTreg cells possess different cell fates despite their comparable in vitro suppressive activity when assessed separately.

In Vivo Conversion of rTreg Cells to aTreg Cells and Differentiation of a Small Fraction of FoxP3⁻ Cells to FoxP3+ Cells

Next, to investigate whether the in vitro conversion of rTreg cells to aTreg cells could also occur in vivo, we transferred human PBMCs containing CFSE-labeled $CD4^+$ T cells into NOG (Nod-scid-common γ-chain-deficient) mice and analyzed their splenocytes 5 days after transfer (Hiramatsu et al., 2003). Fox-$P3^{hi}CD4^+$ T cells recovered in the recipients were largely $CD25^{hi}$ and $CD45RO^+$ (data not shown) and mostly confined to Ki-67^+CFSE-diluting cells, which had divided more than 6 times after transfer (Figure 4A). In addition, most $CD4^+$ T cells expressing low amounts of FoxP3 had not proliferated. These findings correspond to the in vitro findings that $FoxP3^{hi}$ aTreg cells found in PBMCs were highly proliferative and that $FoxP3^{lo}CD4^+$ T cells were Ki-67^- in PBMCs (Figure 1E), suggesting that, upon activation, rTreg cells upregulate FoxP3 expression and then proliferate. We also examined the behavior of Treg cells or whole $FoxP3^+$ cells when injected without other effector $CD4^+$ T cells. Neither population proliferated, indicating that the maintenance and proliferation of FoxP3-expressing cells requires the presence of other $CD4^+$ T cells in vivo (Figure S10).

Similar analysis of PBMCs containing CFSE-labeled rTreg cells, prepared as shown in Figure 1A and Figure S1, showed that they proliferated in vivo and upregulated the expression of FoxP3 and CD45RO along several cell divisions (Figure 4B and data not shown). Because most $FoxP3^{hi}$ cells were detected in CFSE-negative cells after transfer of CFSE-labeled $CD4^+$ T cells or rTreg cells (Figures 4A and 4B), we attempted to determine whether rTreg cells were the major source of CFSE-negative $FoxP3^{hi}$ cells. Injection of PBMCs containing CFSE-labeled $CD4^+$ T cells devoid of rTreg cells revealed a much lower number of $FoxP3^{hi}$ cells when compared with injection of whole $CD4^+$ T cells, indicating that most $FoxP3^{hi}$ aTreg cells derive from rTreg cells (Figure 4C).

Further, to investigate whether the conversion of $FoxP3^-$ to $FoxP3^+$ in $CD4^+$ T cells could occur in vivo, we transferred PBMCs containing CFSE-labeled $FoxP3^-$ $CD127^{hi}CD4^+$ T cells together with nonlabeled $FoxP3^+$ cells (as $CD25^{hi}CD127^{lo}$ cells) in NOG mice and examined whether $FoxP3^-CD4^+$ T cells could upregulate FoxP3 in vivo (Figure 4D). Although most CFSE-labeled cells remained $FoxP3^-$, a small number of cells upregulated FoxP3 from low to high amounts. Injection of only CFSE-labeled $CD4^+FoxP3^-$ cells confirmed that a small fraction (<1%) of $CD4^+FoxP3^-$ cells indeed divided at least 6 times to give rise to $FoxP3^{hi}$ cells (Figure 4E). Taken together, these results indicate that rTreg cells convert to aTreg cells and that only a small fraction of aTreg cells derives from $FoxP3^-CD4^+$ non-Treg cells in vivo.

In Vivo Conversion of rTreg Cells to aTreg Cells in a Normal Human Individual

To obtain further evidence for the in vivo rTreg to aTreg cell conversion in normal humans, we attempted to trace clonotypes of each Treg cell fraction in a single individual at separate time points. Cells in rTreg cells (Fr. I), aTreg cells (Fr. II), and also $FoxP3^-$ non-Treg $CD4^+$ T cells (Fr. IV, V, VI) that expressed the same TCRBV5 family were sorted from a single healthy individual at 18 month intervals. Single-cell RT-PCR and DNA sequencing of the amplicons was performed to compare TCRBV5 CDR3 regions in each sorted subset. Given the small size of the sample, the analysis was able to monitor dominant clones only. First, we observed that rTreg (Fr. I) and aTreg (Fr. II) cell subsets shared few dominant clonotypes at a given time point. Second, we found that a clonotype initially detected in the rTreg cell subset was found dominant 18 months later in the aTreg but not in the rTreg cell subset. The TCR repertoire being potentially so heterogeneous and the sample size being so limited (45 to 137 cells analyzed in each subset), it is highly improbable that T cell clones with identical TCR sequences could be found in the same subsets only by chance. Indeed, when random samples of conventional $CD4^+$ T cells were similarly compared, shared clonotypes were never found in this individual (Figure 5; Table S2). The analysis also revealed that none of the clonotypes found in $FoxP3^-$ cells was found in aTreg cells 18 months later, indicating that if conversion of $FoxP3^-CD4^+$ T cells ever occurs in vivo, it may not be a frequent phenomenon compared with the conversion of rTreg cells to aTreg cells (Figure 5).

Based on these observations in Figures 4 and 5, we conclude that most $FoxP3^{hi}$ aTreg cells are derived from recently activated and vigorously proliferating rTreg cells, and that only a minority of aTreg cells can develop from $FoxP3^-CD4^+$ non-Treg cells in vivo. The result also indicates that the TCR repertoire of Treg cells, in particular that of aTreg cells, adaptively changes in normal individuals.

Variations in Human rTreg and aTreg Cell Populations under Normal and Disease Conditions

We then attempted to determine whether the dissection of $FoxP3^+$ T cells in adult humans into Fr. I–III based on CD45RA and FoxP3 expression was pertinent to the analysis of the dynamics of Treg cell generation and differentiation in ontogeny, aging, and disease states.

Although rTreg cells were highly prevalent in cord blood, we could easily detect Ki-$67^+FoxP3^{hi}CD45RA^-CD4^+$ T cells that corresponded to aTreg cells in adults. We failed to confirm the previously reported finding that all $CD25^+CD4^+$ T cells were $FoxP3^+$ in cord blood (Fritzsching et al., 2006). However, $CD4^+$ T cells expressing the highest amounts of CD25 contained only $FoxP3^+$ cells and CD127 expression efficiently separated $FoxP3^+CD25^+$ from $FoxP3^-CD25^+CD4^+$ T cells (Figure 6A). IFN-γ production was barely detectable in whole $CD4^+$ T cells whereas IL-2 production was observed in $FoxP3^{lo}CD45RA^-CD4^+$ T cells as in adults (data not shown).

Analysis of the expression of CD31 (PECAM-1), which is known to be expressed in recent thymic emigrants but lost during their post-thymic peripheral expansion (Kimmig et al., 2002), revealed that almost all $CD31^+FoxP3^+CD4^+$ T cells in adult PBL were confined in the $CD45RA^+FoxP3^{lo}$ population (Fr. I). This finding suggests that the majority of rTreg cells may be recently derived from the thymus (Figure 6B).

The proportion of rTreg cells (Fr. I) among $CD4^+$ T cells was decreased in aged donors (1.1% ± 0.59%, n = 12 versus 2.40% ± 0.89% in healthy donors, n = 29; $p < 0.0001$) whereas that of aTreg cells (Fr. II) was increased (2.48% ± 1.07% versus 1.63% ± 0.53%; $p = 0.01$; Figures 6C and 6D).

We next applied our new definition of $FoxP3^+$ T cell subsets to the analysis of two pathological conditions that reportedly show

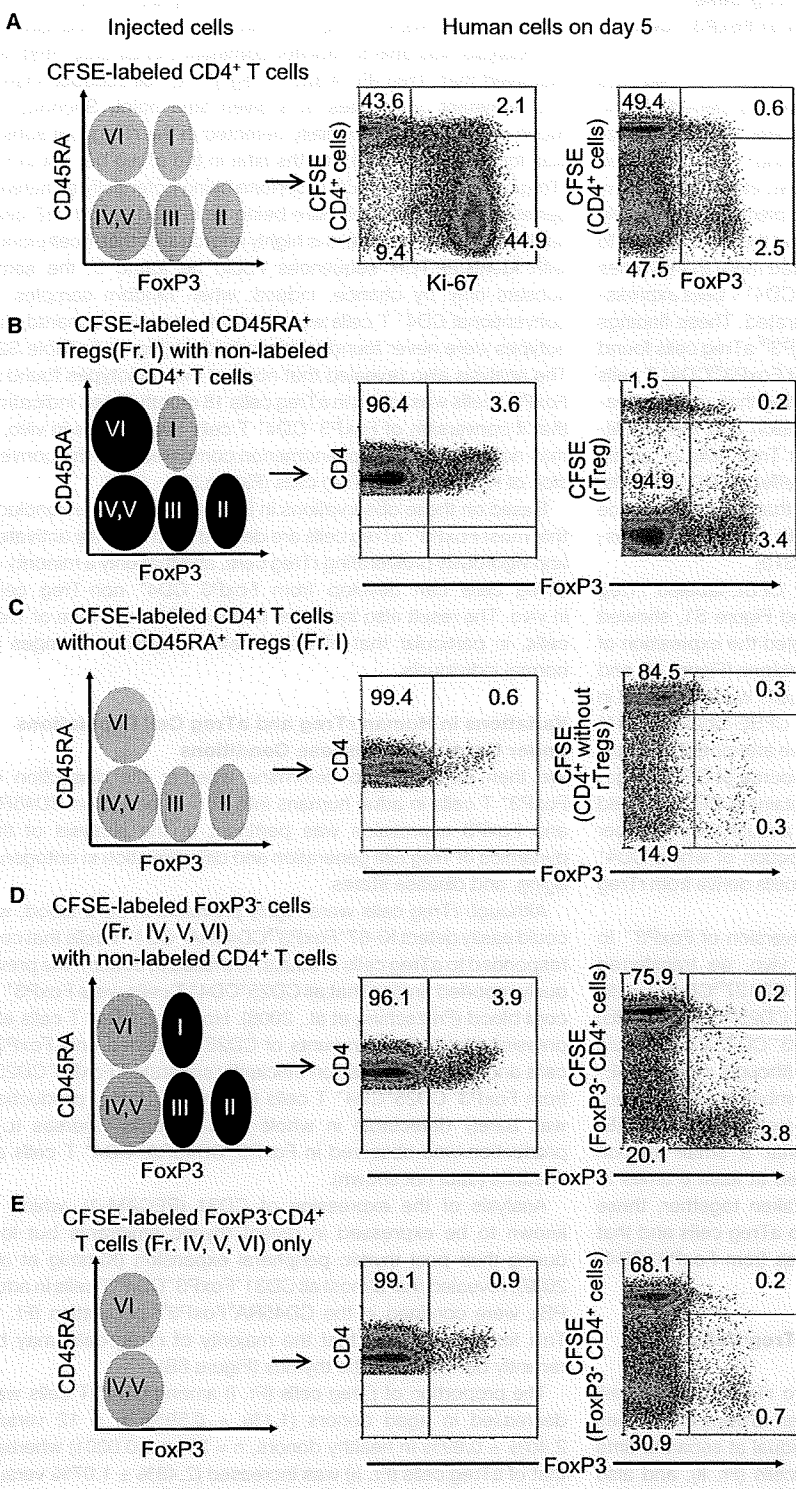

Figure 4. In Vivo Conversion of Treg Cell Phenotype in NOG Mice

PBMCs containing human CD4+ T cells were i.v. injected in NOG mice and collected in the spleen 5 days later. In schematic representations (left) of flow cytometric profiles of injected cells before transfer, CFSE-labeled CD4+ T subsets are depicted in green and injected with nonlabeled cells in black. Flow cytometry of human CD4+ T cells in the spleen after transfer of PBMCs containing CFSE-labeled human whole CD4+ T cells (A) or indicated CFSE-labeled CD4+ T cell subpopulations (B–E) into NOG mice. Numbers indicate percentage in each quadrant (right). Representative data of four mice transferred with PBMCs containing CFSE-labeled CD4+ T cells isolated from three different donors (A), and mice (two for each condition) transferred with PBMCs with indicated CFSE-labeled T cell populations obtained from two different donors (B–E).

different patterns of Treg cell involvement (Miyara et al., 2005, 2006). In sarcoidosis, a granulomatous disease of unknown origin, patients with active disease showed a considerable increase in the proportion of aTreg cells among CD4+ T cells (4.67% ± 3.35%, n = 41; $p < 0.0001$) combined with a high prevalence of Ki-67+FoxP3^{hi}CD4+ T cells and a decrease in the proportions of rTreg cells (1.48% ± 0.89%; $p < 0.0001$). In active systemic lupus erythematosus (SLE), a prototype of systemic autoimmune disease, there was a decrease in the proportion of aTreg cells (1.24 ± 0.72; n = 15; $p = 0.006$) and an increase in the proportions of rTreg cells (4.2 ± 1.86; $p = 0.0008$). Notably, CD45RA$^-$FoxP3^{lo} non-Treg cell fraction (Fr. III) increased to form a distinct population in active SLE (10.37% ± 9.3% versus 3.04 ± 1.1 in healthy donors; $p < 0.0001$; Figures 6C and 6D).

Thus, distinction of Treg cell subsets simply based on the combination of CD45RA and FoxP3 expression is highly informative in assessing the dynamics of Treg cell differentiation under physiological and disease conditions.

DISCUSSION

We have shown in this report that FoxP3+ cells in human PBL are heterogeneous in function and include not only suppressive T cells but also nonsuppressive ones that abundantly secrete proinflammatory cytokines such as IL-17. Further, Treg cells functionally and phenotypically differentiate within the FoxP3+ population. This functional heterogeneity and differentiation dynamics can be clearly shown by separating FoxP3+ cells into three subsets based on the expression of FoxP3 and CD45RA (or CD45RO), which